World Journal of Pharmaceutical Science and Research

www.wjpsronline.com

Research Article

ISSN: 2583-6579
SJIF Impact Factor: 6.916
Year - 2026
Volume: 5; Issue: 2
Page: 05-37

SYNTHESIS, CHARACTERIZATION AND ELUCIDATION OF ANTIMICROBIAL POTENCY OF IRON AND MANGANESE COMPLEXES OF CONDENSATES OF SALICYLALDEHYDE AND 2-HYDROXY ANILINE

Stanley E. Anumata[1*], Uche G. Nwokeke[2], Linus O. Ezenweke[3], Eugenia N. Orjiako[3], Cornelius C. Ahanotu[4,5] and Glory J. Okore[6]

[1]Department of Chemistry/Biochemistry, Federal Polytechnic Nekede, P.M.B 1036, Owerri, Nigeria.
[2]Department of Chemistry, Imo State University, P.M.B 2000, Owerri, Nigeria.
[3]Department of Pure and Industrial Chemistry, Chukwuemeka Odumegwu Ojukwu University, P.M.B 02, Uli, Anambra State, Nigeria.
[4]Department of Science Laboratory Technology, Imo State Polytechnic, Omuma, Oru-East, P.M.B 1472, Owerri, Nigeria.
[5]Basic Science Directorate, Claretian University of Nigeria, Nekede, P.M.B 1019, Owerri, Nigeria.
[6]Department of Chemistry, Alvan Ikoku Federal University of Education, P.M.B 1033, Owerri, Nigeria.

Article Received: 10 December 2025 | | Article Revised: 31 December 2025 | | Article Accepted: 20 January 2026

***Corresponding Author: Stanley E. Anumata**
Department of Chemistry/Biochemistry, Federal Polytechnic Nekede, P.M.B 1036, Owerri, Nigeria.
DOI: https://doi.org/10.5281/zenodo.18438315

How to cite this Article: Stanley E. Anumata, Uche G. Nwokeke, Linus O. Ezenweke, Eugenia N. Orjiako, Cornelius C. Ahanotu and Glory J. Okore (2026) SYNTHESIS, CHARACTERIZATION AND ELUCIDATION OF ANTIMICROBIAL POTENCY OF IRON AND MANGANESE COMPLEXES OF CONDENSATES OF SALICYLALDEHYDE AND 2-HYDROXY ANILINE. World Journal of Pharmaceutical Science and Research, 5(2), 05-37. https://doi.org/10.5281/zenodo.18438315

ABSTRACT
This study sought to synthesize and characterize iron and manganese complexes of 2-Phenyliminomethylphenol (PMP) and 2,2-hydroxybenzylideneaminophenol (HAP) as well as their mixed ligand complexes, and to elucidate their antimicrobial potency against microbes. The PMP and HAP were synthesized by reacting aniline and 2-aminophenol with salicylaldehyde respectively. The preparation of the unmixed metal complexes were achieved by adding 0.29mmol 2-Phenyliminomethylphenol ligand into the appropriate metal salt in the one hand, and by adding 0.29mmol 2,2-hydroxybenzylideneaminophenol ligand into the appropriate metal salt in the other hand, while the mixed metal complexes were prepared by addition of equimolar amount of ligands of 2-Phenyliminomethylphenol and 2,2-hydroxybenzylideneaminophenol into the appropriate metal salt. The molecular structures of the ligand and their complexes were determined using GC-MS, FTIR, UV-Vis, ^{1}HNMR, and X-Ray diffraction studies. The melting point and solubility of the synthesized ligands and complexes were determined using standard methods. All complexes and ligands were found to be soluble in dimethylsulfoxide (DMSO). Asymmetric octahedral geometry was observed for all complexes with PMP, HAP, and mixed ligands. A bidentate ligand is coordinated to metal ions through oxygen atoms of carbonyl groups and nitrogen atoms of two imine groups for the metal complexes. Except for the mixed ligand complex of Fe (II), the XRD pattern indicates that the ligand and metal complexes are crystalline with high crystallite size of 119.23nm to 638.67nm. The XRD results indicate the crystal formed by the ligands and their respective complexes are large. However, the ligands had higher size compared to the complexes formed, which could be due to the complexation reactions. X-ray diffractograms of the metal complexes investigated showed good intense peaks indicating high crystallinity except for mixed ligand (PMP+HAP) complexes of iron [Fe(PMP+HAP).Cl_2] with reduced and broadened peak indicating reduced crystallinity. The FTIR spectra of 2-Phenyliminomethylphenol (PMP) indicated absorbance at 1569.2 cm^{-1} suggesting the stretching C=C bond in the benzene rings, while absorptions recorded at 1613.9 cm^{-1} suggested the =C-N stretching in the benzene ring. The electronic spectra of the complexes formed showed energy absorbed in the ultraviolet/visible region produced changes in the electronic energy of the compound resulting from transition of valence electrons in the complexes. Antimicrobial screening were carried with ligands PMP and HAP and the metal complexes using clinical isolates of Gram Positive Bacteria (*Staphylococcus aureus* and *Bacillus substilis*), Gram Negative Bacteria (*Escherichia coli* and *Pseudomonas aeruginosa*) and Fungi (*Candida albicans* and *Aspergillus niger*). The ligand of 2-PMP and 2,2-HAP showed partial inhibitory action on the clinical isolates of Gram Postive, Gram Negative and no inhibitory action on the Fungi while metal complexes of Mn(II) with both mixed and unmixed ligands showed either strong or stronger inhibition on the clinical isolates of Gram Positve, Gram Negative and Fungi isolates. The study concludes that the synthesized ligands and complexes are soluble in dimethylsulfoxide (DMSO) but solubility varied with respect to other solvents. Also, all the complexes were purely crystalline as revealed by the results, and exhibited inhibitory actions on Gram Positive bacteria, Gram Negative bacteria and Fungi species.

KEYWORDS: Fe(II) complex, Mn(II) complex, 2-Phenyliminomethylphenol, 2,2-ydroxybenzylideneaminophenol, Metal complexes.

1. INTRODUCTION

In inorganic chemistry, a complex is a chemical compound whose structure comprises of a central metal ion with coordinate covalent bonds to one or more ligands. Since ligands donate pairs of electrons, hence they are classified as Lewis bases. Conversely, central metal ions which accept pairs of electrons are referred to as Lewis acids. The nature of metal–ligand bonding can range from covalent to ionic (Hartwig *et al.*, 2010). Furthermore, the metal–ligand bond order can range from one to three. Metals and metalloids are bound to ligands in almost all condition due to affinity to donate pair of electrons. Ligands in a complex dictate the reactivity of the central metal atom, including ligand substitution rates, the reactivity of the ligands themselves, and redox (Miessler *et al.*, 2014). This allows the ligand to coordinate (or bind) to the central atom or ion, creating a coordination complex. Ligands are typically Lewis bases, which means that they have at least one pair of non-bonded electrons that it can use to form a bond with the central atom or ion. This allows the ligand to coordinate (or bind) to the central atom or ion, creating a coordination complex, furthermore ligands play a key role in coordination chemistry, allowing the formation of complex molecules and ions with a wide range of properties and applications.

One important feature of metal complexes is the coordination number. The coordination number of a complex is the number of ligand-binding sites on the metal ion. The bond between the metal ion and the ligand, where the ligand supplies both electrons, is known as a co-ordinate covalent (or dative covalent) bond (Anumata *et al.*, 2024). In this type of covalent bond, the shared pair of electrons originate from only one of the participating atoms. Transition metals involved in complex ions have two sets of valence electrons participating in bonding. The first set of bonding electrons is called primary valence, and it is the oxidation number of the metal. The oxidation number can be determined by looking at the charge on the transition metal ion. Copper (Cu), for example, has an oxidation number/state of +2. Sometimes this number must be inferred based on the overall charge of the complex ion. The primary valence electrons are involved in typical ionic bonds (Hartwig, 2010). The second set of transition metal valence electrons are called secondary valence, usually referred to as the coordination number. The secondary valence electrons are involved with bonding to the ligands. The coordination number indicates the number of ligands that a metal ion is bonded to. Ligands bond to transition metals by sharing a lone pair of electrons. This type of interaction is a Lewis acid-base reaction, where the metal ion is the Lewis acid and the ligand is the Lewis base. The resulting bond in which one species donates both bonding electrons is called a coordinate covalent bond (Kay *et al*., 2000).

Among the essential properties of coordination compounds are the number and arrangement of the ligands attached to the central metal atom or ion—that is, the coordination number and the coordination geometry, respectively (Anumata *et al.*, 2024). Coordination numbers are also affected by the 18-electron rule sometimes referred to as noble gas rule, which states that coordination compounds in which the total number of valence electrons approaches but does not exceed 18 (the number of electrons in the valence shells of the noble gases) are most stable. The stabilities of 18-electron valence shells are also reflected in the coordination numbers of the stable mononuclear carbonyls of different metals that have oxidation number 0 for instance, tetracarbonylnickel, pentacarbonyliron, and hexacarbonylchromium, each of which has a valence shell of 18. The 18-electron rule applies particularly to covalent complexes, such as the cyanides, carbonyls, and phosphines. For more ionic also called outer-orbital complexes, such as fluoro or aqua complexes, electronic factors are less important in determining coordination numbers, and configurations corresponding to more than 18 valence electrons are not uncommon. Several nickel (+2) complexes, for example – including the hexafluoro, hexaaqua, and hexaamine complexes—each have 20 valence electrons (Ahmad *et al*., 2016).

Any one metal ion tends to have the same coordination number in different complexes for example, generally six for chromium (+3) – but this is not invariably so. Differences in coordination number may result from differences in the sizes of the ligands; for example, the iron (+3) ion is able to accommodate six fluoride ions in the hexafluoro complex $[FeF_6]>]^{3-}$ but only four of the larger chloride ions in the tetrachloro complex $[FeCl_4]^-$. In some cases, a metal ion and a ligand form two or more complexes with different coordination numbers—e.g., tetracyanonickelate $[Ni(CN)_4]>]^{2-}$ and pentacyanonickelate $[Ni(CN)_5]>]^{3-}$, both of which contain Ni in the +2 oxidation state (Lawal *et al*., 2015).

The coordination chemistry of metal complexes plays a vital role in biological system of organisms as well as in chemical processes. Transition metal complexes are important in catalysis, material synthesis, photochemistry and biological systems. The synthesis of ternary complexes mainly involves the interaction of metal ion with two or more different ligands. Recently there has been considerable interest in mixed chelation as it occurs commonly in biological fluids, which contain millions of potential ligands that are likely to compete *in vivo* for metal ions. It is well known that the ternary coordination complexes play an important role in biological processes as exemplified by many instances in which enzymes are known to be activated by metal ions (Sherif & Eldebss, 2011). Ternary complexes have also been implicated in the storage and transport of active substances through membranes (Reddy & Rao, 2006) and these phenomena are strongly dependent on the formation of these species and the electronic configuration of metal ion concerned. In this study, the scholars sought to synthesize and characterize iron and manganese complexes and mixed ligand complexes of 2-phenyliminomethylphenol (PMP) and 2,2-hydroxybenzylideneaminophenol (HAP) and to elucidate the antimicrobial potency of these complexes against microbes.

2. Experimental Procedures

2.1 Synthesis of the two ligands – PMP and HAP

The two ligands used in this study were 2-phenyliminomethylphenol (PMP) and 2,2-hydroxybenzyleneaminophenol (HAP). The procedures adopted in their synthesis have been previously reported (Anumata *et al.*, 2024; Anumata *et al.*, 2025).

2.2 Synthesis of mononuclear metal ligand complexes of PMP

The Fe(II) and Mn(II) complexes were prepared following a method earlier reported by Anumata *et al.* (2024; 2025) by adding 2-phenyliminomethylphenol ligand (0.29 mmol) into ethanol (30 ml) followed by 0.22 g (1 mmol) of the metal salts ($FeCl_2$ and $MnCl_2$) respectively. The solution was properly mixed and heated under reflux conditions and allowed to cool. The crystals were then collected and purified by washing with ethanol and diethyl ether and finally air dried.

2.3 Synthesis of mononuclear metal ligand complexes of HAP

The Fe(II) and Mn(II) complexes were prepared following a similar procedure reported by Anumata *et al.* (2024, 2025). The 2,2-hydroxybenzylideneaminophenol ligand (0.29 mmol) were added into 30 mL of ethanol followed by 0.22 g (1 mmol) of the metal salts ($FeCl_2$ and $MnCl_2$) respectively. The resultant solution was thoroughly mixed refluxed and allowed to cool afterwards. The crystals were then collected and washed with ethanol and diethyl ether and finally air dried.

2.4 Synthesis of mononuclear metal mixed ligand complexes of PMP and HAP

Following a procedure previously reported (Anumata *et al.*, 2024; Anumata *et al.*, 2025), the mononuclear mixed ligand complexes of Fe(II) and Mn(II) were synthesized by adding 0.29 mmol of 2-phenyliminomethehylphenol ligand

(PMP) and 0.29 mmol of 2,2-hydroxybenzylideneaminophenol (HAP) into 30 mL of ethanol, followed by 0.22 g (1 mmol) respectively of the metal salts ($FeCl_2$ and $MnCl_2$. The resulting solution was thoroughly mixed and refluxed at 60°C for 3 hours and allowed to cool. Crystals were then collected, purified by washing with ethanol and diethyl ether and then air dried.

2.5 Molar conductivity and chemical analyses of synthesized metal complexes

The molar conductivity of all the complexes were measured using conductivity meter of Model EQ664 with inbuilt magnetic stirrer as previously reported elsewhere (Anumata *et al.* 2024; Anumata *et al.*, 2025). The infrared spectra of the ligands and complexes, the UV analysis, X-Ray diffraction analysis of the mixed ligand complexes powder form, ^{1}H-NMR spectral analysis, and GC-MS analysis were all recorded as previously reported using the same instruments (Anumata *et al.* 2024; Anumata *et al.*, 2025).

2.6 Antimicrobial screening

In this screening, the clinical isolates of *Staphylococcus aureus* and *Bacillus substilis* representative of Gram Positive Bacteria, *Escherichia coli* and *Pseudomonas aeruginosa* representative of Gram Negative Bacteria, and *Candida albicans* and *Aspergillus niger* representative of Fungi were collected and sub-cultured on sterile nutrient agar. The antimicrobial analysis were carried out following the procedure that has been reported previously (Anumata *et al.* 2024; Anumata *et al.*, 2025) and observations were recorded.

3. RESULTS AND DISCUSSION

3.1 Melting point and solubility characterization of metal complexes

The melting point and solubility characteristics of the prepared ligands and their complexes are presented in Table 1 that follows, while the solubility characteristics are presented in Table 2.

Table 1: Ligands and complexes and their melting points.

Ligands and Complexes	Melting Point
PMP	94°C (Anumata *et al.*, 2024)
HAP	106°C (Anumata *et al.*, 2024)
$[Fe(PMP)_2.Cl_2]$	94°C
$[Fe(HAP)_2.Cl_2]$	70°C
$[Fe(PMP+HAP).Cl_2]$	93°C
$[Mn(PMP)_2.Cl_2]$	95°C
$[Mn(HAP)_2.Cl_2]$	68°C
$[Mn(PMP+HAP).Cl_2]$	96°C

The melting points of metal complexes indicate the strength of the metal-ligand bond and it can also be deployed to assess the purity of the complex. The melting points of the synthesized complexes in this study were very comparable to that of the ligand PMP with the exception of $[Fe(HAP)_2.Cl_2]$ and $[Mn(HAP)_2.Cl_2]$ which has melting points of 70^0C and 68^0C respectively. However, all the complexes have melting points lower than that of the ligand HAP.

Table 2: Melting point and solubility values of the metal complexes.

	Melting Point	Ac	MeOH	EtOH	Diethyl-ether	N-Hexane	CCl_4	Water	CS_2	DMSO
PMP	94°C	SS	SS	SIS	SS	IS	SIS	IS	SS	SS
HAP	106°C	SS	MS	SIS	MS	IS	IS	IS	SIS	SS
$[Fe(PMP)_2.Cl_2]$	94°C	IS	IS	IS	SIS	IS	IS	IS	IS	SS

[Fe(HAP)$_2$.Cl$_2$]	70°C	MS	SIS	IS	IS	IS	IS	IS	IS	SS
[Fe(PMP+HAP).Cl$_2$]	93°C	MS	SIS	IS	IS	IS	IS	IS	IS	SS
[Mn(PMP)$_2$.Cl$_2$]	95°C	SIS	IS	IS	IS	IS	IS	IS	IS	SS
[Mn(HAP)$_2$.Cl$_2$]	68°C	IS	IS	IS	IS	IS	IS	IS	IS	SS
[Mn(PMP+HAP)$_2$.Cl$_2$]	96°C	IS	IS	IS	IS	IS	IS	IS	IS	SS

SS: Strongly Soluble; MS**:** Moderately Soluble; IS: Insoluble; SIS**:** Slightly Soluble

From Table 2, it can be observed that all synthesized complexes and their ligands were strongly soluble in dimethylysulfoxide (DMSO) but insoluble in n-Hexane and water. In general, over 85% of the metal complexes and their mixed ligand complexes showed insolubility across all solvents except in DMSO. Both PMP and HAP (ligands) also showed strong solubility in acetone, while only the mixed ligand complex of Fe was moderately soluble in acetone.

3.2 NMR Analysis

The NMR spectral data for the ligands have been reported elsewhere (Anumata *et al.*, 2024) and are presented in Appendix B.

3.3 GC-MC Analysis

The results of the Gas Chromatography-Mass Spectrometry (GC-MS) analysis are presented in Tables 3–10 while the chromatograms are shown in Appendix D (a–f). Data from the GC-MS analysis reveal that the detected compounds/fragments possess an unsaturated phenolic moiety, an indication of potential activity. Again, identification of these GC-MS fragmented compounds in the complexes serves as the basis for the determination of bioactive therapeutic constituents present and other possible health benefits of the metal complexes, leading to further pharmaceutical and biological studies regarding their anticancer, antimutagenic, antitumor and anti-inflammatory applications (Anumata *et al.*, 2024; Anumata *et al.*, 2025).

Table 3: GC-MS fragments of sample A (PMP); Molecular ion of 2-Phenyliminomethylphenol (PMP) = 197.23g/mol.

S/N	RT	Area (Pct)	Name of Compound	*m/z*	Mol. Weight	Mol. Formula
1	7.115	67,000	Mercaptamine	59	77.149g/mol	C_2H_7NS
2	9,909	45,000	Aniline	97	93.13 g/mol	$C_6H_5NH_2$
3	11.718	97,000	Benzaldehyde, 2-hydroxy-	96	122.1213g/mol	$C_7H_6O_2$
4	12.360	97,000	Benzaldehyde, 2-hydroxy-	94	122.1213g/mol	$C_7H_6O_2$
5	16.017	52,000	Fumaramic acid	37	116.07g/mol	$C_4H_4O_4$
6	20.978	102,000	Propanamide, N-acetyl-N-(3-Methylbutyl) acetamide	38	129.2001g/mol	$C_7H_{15}NO$
7	22.142	96,000	Decane	64	142.28g/mol	$C_{10}H_{22}$
8	26.493	120,000	7-Heptadecene, 1-chloro-	30	272.9g/mol	$C_{17}H_{33}Cl$
9	31.723	803,000	Salicylidene aniline	98	**197.23g/mol**	$C_{13}H_{11}NO$
10	32.094	11,000	Salicylidene aniline	95	197.23g/mol	$C_{13}H_{11}NO$
11	32.642	48,000	Hexadecanoic acid, ethyl ester	90	284.4772g/mol	$C_{18}H_{36}O_2$
12	33.487	726,000	9-Octadecenoic acid (Z)-, 2-hydroxy-1-(hydroxymethyl)ethyl ester	93	356.5g/mol	$C_{21}H_{40}O_4$
13	33.653	559,000	17-Pentatriacontene	96	490.9303g/mol	$C_{35}H_{70}$
14	33.989	115,000	9-Octadecenoic acid	94	282.5g/mol	$C_{18}H_{34}O_2$
15	34.172	46,000	5-Eicosene, (E)-	78	280.5316g/mol	$C_{20}H_{40}$
16	34.287	240,000	9-Octadecenamide, (Z)-	95	281.4766g/mol	$C_{18}H_{35}NO$
17	34.970	67,000	9-Octadecenoic acid (Z)-, 2,3-dihydroxypropyl-ester	90	356.5399g/mol	$C_{21}H_{40}O_4$

18	35.097	133,000	1H-Indene, 5-butyl-6-hexyloctahydro-	60	264.5g/mol	$C_{19}H_{36}$
19	35.912	3,999,000	9-Octadecenamide, (Z)-	98	281.4766g/mol	$C_{18}H_{35}NO$
20	36.138	383,000	Octadecanamide	93	283.5g/mol	$C_{18}H_{37}NO$
21	36.766	1,997,000	Oleic Acid	80	282.5g/mol	$C_{18}H_{34}O_2$

Table 4: Showing GC-MS fragments of Sample B (HAP); Molecular Ion of 2,2-Hydroxybenzylideneaminophenol (HAP) = 214.34g/moL.

S/N	RT	Area (Pct)	Name of Compound	*m/z*	Mol. Weight	Mol. Formula
1	5.817	267,000	2-Hexanol, 3-methyl-	53	116.2013g/mol	$C_7H_{16}O$
2	10.888	209,000	Ethanol, 2-bromo-	38	124.96g/mol	C_2H_5BrO
3	13.522	162,000	3-Pentanone, dimethylhydrazone	50	128.22g/mol	$C_7H_{16}N_2$
4	20.845	246,000	4-Hexenoic acid, 6-hydroxy-4-methyl-, methyl ester, (E)-	40	158.19g/mol	$C_8H_{14}O_3$
5	32.7164	1,144,360	Undecanoic acid, ethyl ester	49	**214.3443g/mol**	$C_{13}H_{26}O_2$
6	29.087	863,000	2-Methyl-Z,Z-3,13-octadecadienol	78	280.5g/mol	$C_{19}H_{36}O$
7	32.094	37,000	Hexadecanoic acid, methyl ester	68	270.4507g/mol	$C_{17}H_{34}O_2$
8	32.643	90,000	Hexadecanoic acid, ethyl ester	64	284.4772g/mol	$C_{18}H_{36}O_2$
9	33.482	220,000	9,17-Octadecadienal, (Z)-	83	264.4g/mol	$C_{18}H_{32}O$
10	33.674	46,000	Heptadecanoic acid, heptadecyl ester	55	354.6g/mol	$C_{23}H_{46}O_2$
11	34.000	187,000	9-Octadecenoic acid	95	282.5g/mol	$C_{18}H_{34}O_2$
12	34.179	106,000	Oleic Acid	41	282.5g/mol	$C_{18}H_{34}O_2$
13	35.107	1,098,000	Octadecanal	83	268.4778g/mol	$C_{18}H_{36}O$
14	35.755	6,420,000	17-Pentatriacontene	95	490.9303g/mol	$C_{35}H_{70}$
15	36.772	51,000	cis-13-Octadecenoic acid	53	282.5g/mol	$C_{18}H_{34}O_2$

Table 5: Showing GC-MS fragments of Sample O [$Fe(PMP)_2.Cl_2$], molecular ion of [$Fe(PMP)_2.Cl_2$] = 520.845g/mol.

S/N	RT	Area (Pct)	Name of Compound	*m/z*	Mol. Weight	Mol. Formula
1	10.011	914,000	Aniline	97	93.13 g/mol	$C_6H_5NH_2$
2	11.781	140,000	Benzaldehyde, 2-hydroxy-	95	122.1213g/mol	$C_7H_6O_2$
3	17.134	211,000	Benzeneacetic acid, 2-hydroxy-	47	152.1473g/mol	$C_8H_8O_3$
4	25.792	452,000	Oleic Acid	41	282.46g/mol	$C_{18}H_{34}O_2$
5	30.786	8,000	2-Piperidinone, N-[4-bromo-n-butyl]	43	234.13g/mol	$C_9H_{16}BrNO$
6	31.674	2,213,000	Salicylidene aniline	98	197.23g/mol	$C_{13}H_{11}NO$
7	32.100	904,000	Hexadecanoic acid, methyl ester	93	270.4507g/mol	$C_{17}H_{34}O_2$
8	32.463	4,887,000	Cyclotetradecane, 1,7,11-trimethyl-4-(1-methylethyl)-	90	280.5316g/mol	$C_{20}H_{40}$
9	33.484	149,000	9-Octadecenoic acid (Z)-, methyl ester	87	296.4879g/mol	$C_{19}H_{36}O_2$
10	33.663	36,000	Methyl 8,10-dimethyl-hexadecanoate	89	569.0g/mol	$C_{36}H_{72}O_4$
10	33.842	113,000	2,2-diaminodichloroHeptacosanoic acid	78	**520.845g/mol**	$C_{27}H_{33}Cl_2N_2O_4$
11	33.999	64,000	3-Eicosene, (E)-	93	280.5g/mol	$C_{20}H_{40}$
12	34.177	32,000	Octadecanoic acid, ethyl ester	80	312.5304g/mol	$C_{20}H_{40}O_2$
13	35.962	13,000	Oleic Acid	80	282.46g/mol	$C_{18}H_{34}O_2$
14	36.826	-22,000	Oleic Acid	55	282.46g/mol	$C_{18}H_{34}O_2$
14	36.826	-22,000	Oleic Acid	55	282.46g/mol	$C_{18}H_{34}O_2$

Table 6: Showing GC-MS fragments of Sample P [$Fe(HAP)_2.Cl_2$], molecular ion of [$Fe(HAP)_2.Cl_2$] = 554.84g/mol.

S/N	RT	Area (Pct)	Name of Compound	*m/z*	Mol. Weight	Mol. Formula
1	7.518	255,000	Butane, 1,1-diethoxy-	43	146.2273g/mol	$C_8H_{18}O_2$
2	13.283	215,000	7-Hydroxy-3-(1,1-dimethylprop-2-enyl) coumarin	35	230.26g/mol	$C_{14}H_{14}O_3$
3	14.589	145,000	3-Pentanone, dimethylhydrazone	30	128.22 g/mol	$C_7H_{16}N_2$
4	18.110	200,000	Acetic acid, cyano-	38	85.0614g/mol	$C_3H_3NO_2$

5	19.428	149,000	5-Dimethylamino-1-penten-3,5-dione	43	157.25300g/mol	$C_9H_{19}NO$
6	24.207	286,000	N-Methoxy-1-ribofuranosyl-4-imidazolecarboxylic amide	35	273.24 g/mol	$C_{10}H_{15}N_3O_6$
7	28.169	281,000	9,12-Octadecadienoic acid (Z,Z)-	58	280.4455g/mol	$C_{18}H_{32}O_2$
8	30.789	180,000	1-Decanol, 2-octyl-	30	270.5g/mol	$C_{18}H_{38}O$
9	32.271	7,891,000	Oleic Acid	66	282.46g/mol	$C_{18}H_{34}O_2$
10	33.479	228,000	cis-Vaccenic acid	91	282.5g/mol	$C_{18}H_{34}O_2$
11	33.996	115,000	Ethyl 9-hexadecenoate	93	282.4614g/mol	$C_{18}H_{34}O_2$
12	34.173	57,000	Octadecanoic acid, ethyl ester	96	312.5304g/mol	$C_{20}H_{40}O_2$
13	34.350	58,000	3,4-diaminodichloro(Nonacosanoic acid)	98	**554.845g/mol**	$C_{29}H_{43}Cl_2N_2O_4$

Table 7: Showing GC-MS fragments of Sample Q [Fe(PMP+HAP).Cl_2], molecular ion of [Fe(PMP+HAP).Cl_2] = 537.84g/mol.

S/N	RT	Area (Pct)	Name of Compound	*m/z*	Mol. Weight	Mol. Formula
1	7.213	266,000	2-Isopropoxyethylamine	27	103.16g/mol	$C_5H_{13}NO$
2	14.365	156,000	Pyridine, 2-methyl-	30	93.13g/mol	C_6H_7N
3	20.518	383,000	Pterin-6-carboxylic acid	25	207.15g/mol	$C_7H_5N_5O_3$
4	22.940	307,000	6,7-Dioxabicyclo[3.2.2]nonane	35	128.17g/mol	$C_7H_{12}O_2$
5	29.442	1,038,000	Z-8-Methyl-9-tetradecenoic acid	83	240.3816g/mol	$C_{15}H_{28}O_2$
6	31.693	166,000	Salicylidene aniline	97	197.23g/mol	$C_{13}H_{11}NO$
7	32.092	26,000	Hexadecanoic acid, methyl ester	89	270.4507g/mol	$C_{17}H_{34}O_2$
8	32.640	122,000	Hexadecanoic acid, ethyl ester	95	284.4772g/mol	$C_{18}H_{36}O_2$
9	33.480	175,000	9,17-Octadecadienal, (Z)-	96	264.4g/mol	$C_{18}H_{32}O$
10	33.665	38,000	Oleic Acid	93	282.46g/mol	$C_{18}H_{34}O_2$
11	33.999	198,000	9-Octadecenoic acid	92	282.5 g/mol	$C_{18}H_{34}O_2$
12	34.333	160,000	4,4-diaminodichlorooctacosanoic acid	98	**537.845g/mol**	$C_{28}H_{38}Cl_2N_2O_4$
13	34.176	85,000	Octadecanoic acid, ethyl ester	84	312.5304g/mol	$C_{20}H_{40}O_2$
14	34.307	159,000	Oleic Acid	59	282.46g/mol	$C_{18}H_{34}O_2$
15	35.788	6,774,000	17-Pentatriacontene	94	490.9303g/mol	$C_{35}H_{70}$
16	36.792	73,000	Undec-10-ynoic acid, tetradecyl ester	45	378.6g/mol	$C_{25}H_{46}O_2$
17	37.123	33,000	Oleic Acid	50	282.46g/mol	$C_{18}H_{34}O_2$

Table 8: Showing GC-MS fragments of Sample R [Mn$(PMP)_2$.Cl_2]; molecular ion of [Mn$(PMP)_2$.Cl_2] = 519.93/mol.

S/N	RT	Area (Pct)	Name of Compound	*m/z*	Mol. Weight	Mol. Formula
1	6.0498	1,109,470	Aniline	97	93.13g/mol	C_6H_7N
2	6.9901	182,170	Cyclohexene, 1-methyl-5-(1-methylethenyl)-	43	136.2340g/mol	$C_{10}H_{16}$
3	7.5638	468,760	Benzaldehyde, 2-hydroxy-	96	122.1213g/mol	$C_7H_6O_2$
4	7.7969	284,490	Benzaldehyde, 2-hydroxy-	94	122.1213g/mol	$C_7H_6O_2$
5	8.5826	44,560	Ethyl 3-methyl-8-[p-sulfamylbenzylamino]pyrido	38	[2,3-b]pyrazin-6-carbamate	
6	8.6927	55,050	N,N'-Dicarbethoxy-N-[2,4-diamino-6-hydroxy-5-pyrimidinyl]hydrazine	47	126.11664g/mol	$C_4H_6N_4O$
7	8.7257	47,740	1-Octanamine	35	129.2432g/mol	$C_8H_{19}N$
8	9.3025	83,140	Methanamine, N-1(1-phenylethylidene)-	50	133.19g/mol	$C_9H_{11}N$
9	10.6802	80,060	5-Nonanone, dimethylhydrazone	38	184.32g/mol	$C_{11}H_{24}N_2$
10	11.8578	37,390	Acetic acid, cyano-	38	85.0614g/mol	C_3H_3NO
11	11.9373	94,580	Metanephrine	46	197.23g/mol	$C_{10}H_{15}NO_3$
12	13.0968	32,920	1-Propanamine, N-nitro-	59	104.11g/mol	$C_3H_8N_2O_2$
13	13.1222	10,810	Cyclohexanone, dimethylhydrazone	59	140.23g/mol	$C_8H_{16}N_2$
14	13.1406	30,010	Tetrahydro-4H-pyran-4-ol	22	102.1317g/mol	$C_5H_{10}O_2$
15	14.6372	81,530	N-Methoxy-1-ribofuranosyl-4-imidazolecarboxylic amide	53	273.24g/mol	$C_{10}H_{15}N_3O_6$
16	15.7745	81,590	Tetrahydro-4H-pyran-4-ol	50	102.1317g/mol	$C_5H_{10}O_2$
17	16.7544	30,890	Benzaldehyde, 2-ethoxy-	53	150.1745g/mol	$C_9H_{10}O_2$
18	20.1177	49,130	Norpseudoephedrine	59	151.21g/mol	$C_9H_{13}NO$

19	20.1642	41,350	Bicyclo[6.1.0]nonane, 9-(1-methylethylidene)-	38	164.2872g/mol	$C_{12}H_{20}$
20	20.3517	18,570	Butylated Hydroxytoluene	98	220.35g/mol	$C_{15}H_{24}O$
21	21.2934	47,770	Urea, (trifluoromethyl)-	35	128.053g/mol	$C_2H_3F_3N_2O$
22	21.3094	45,480	2-Formyl-l-tryptophan	38	332.356g/mol	$C_{17}H_{20}N_2O_5$
23	23.2811	35,740	3-Methyl-3,5- -(cyanoethyl)tetrahydro-4-thiopyranone	64	236.34g/mol	$C_{12}H_{16}N_2OS$
24	23.3454	61,400	Piperidine, 3-(bromomethyl)-	64	178.07g/mol	$C_6H_{12}BrN$
25	24.5363	132,370	1,2-Propanediol, 3-chloro	25	110.54 g/mol	$C_3H_7ClO_2$
26	26.752	92,200	E-7-Octadecene	86	252.4784g/mol	$C_{18}H_{36}$
27	26.8249	22,780	Dodecanal	35	184.32g/mol	$C_{12}H_{24}O$
28	28.1881	1,163,300	Salicylidene aniline	99	197.23g/mol	$C_{13}H_{11}NO$
29	28.5894	12,610	Salicylidene aniline	91	197.23g/mol	$C_{13}H_{11}NO$
30	28.6148	11,720	Phenol, 2-[(phenylmethylene)amino]-	95	197.23300g/mol	$C_{13}H_{11}NO$
31	28.6373	8,520	Salicylidene aniline	93	197.23g/mol	$C_{13}H_{11}NO$
32	28.7539	37,170	4-Hydroxybenzalaniline	96	197.2325g/mol	$C_{13}H_{11}NO$
33	28.7702	14,930	Salicylidene aniline	98	197.23g/mol	$C_{13}H_{11}NO$
34	28.8558	92,630	Phenol, 2-[(phenylmethylene)amino]-	90	197.23300g/mol	$C_{13}H_{11}NO$
35	28.8855	78,360	4-Hydroxybenzalaniline	95	197.2325g/mol	$C_{13}H_{11}NO$
36	28.9293	24,720	Salicylidene aniline	95	197.23g/mol	$C_{13}H_{11}NO$
37	28.9455	106,070	Salicylidene aniline	74	197.23g/mol	$C_{13}H_{11}NO$
38	29.2599	34,590	Pentadecanoic acid, 14-methyl-, methyl ester	98	270.4507g/mol	$C_{17}H_{34}O_2$
39	30.017	164,750	Hexadecanoic acid, ethyl ester	98	284.4772g/mol	$C_{18}H_{36}O_2$
40	30.8606	198,540	Cyclotetradecane	41	196.3721g/mol	$C_{14}H_2$
41	30.9015	354,350	9,12-Octadecadienoic acid (Z)-, methyl ester	99	294.4721g/mol	$C_{19}H_{34}O_2$
42	30.944	1,080,060	9,12-Octadecadienoic acid (Z)-, methyl ester	99	294.4721g/mol	$C_{19}H_{34}O$
43	31.1323	52,230	Methyl stearate	95	298.5g/mol	$C_{19}H_{38}O_2$
44	31.4171	279,930	Ethyl Oleate	95	310.5g/mol	$C_{20}H_{38}O_2$
45	31.5867	85,670	Octadecanoic acid, ethyl ester	99	312.5304g/mol	$C_{20}H_{40}O_2$
46	31.8481	1,660	Oleic acid	78	282.46g/mol	$C_{18}H_{34}O_2$
47	31.9007	740	Oleic acid	74	282.46g/mol	$C_{18}H_{34}O_2$
48	31.9915	9,990	Linoleic acid ethyl ester	83	308.4986g/mol	$C_{20}H_{36}O_2$
49	32.0189	14,760	n-Propyl 11-octadecenoate	96	324.5g/mol	$C_{21}H_{40}O_2$
50	32.0995	19,510	Heptadecanal	55	254.5g/mol	$C_{17}H_{34}O$
51	32.2346	69,440	13-Octadecenal, (Z)-	64	266.5g/mol	$C_{18}H_{34}O$
52	32.2688	17,650	Cyclohexane, 1-(1,5-dimethylhexyl)-4-(4-methylpentyl)-	48	280.5316g/mol	$C_{20}H_{40}$
53	32.4807	343,600	11-(2-Cyclopenten-1-y)undecanoic acid, $(_+)$-	48	252.3923g/mol	$C_{16}H_{28}O_2$
54	32.4972	43,310	Hexadecane, 1-(ethenyloxy)-	49	268.485g/mol	$C_{18}H_{36}O$
55	32.5161	47,960	1-Heptadecene	59	238.4519g/mol	$C_{17}H_{34}$
56	32.5905	354,450	6-Octadecenoic acid, (Z)-	55	282.4614g/mol	$C_{18}H_{34}O_2$
57	35.8088	49,720	Squalene	95	410.7g/mol	$C_{30}H_{50}$
58	36.1066	81,870	(2R,3R,4aR,5S,8aS)-2-Hydroxy-4a,5-dimethyl-3-(prop-1-en-2-yl)	46	236.3499g/mol	Octahydronaphthalen-1(2H)-one
59	36.1599	30,360	Oleic acid	50	282.46g/mol	$C_{18}H_{34}O_2$
60	36.2132	51,510	2,2-diaminodichloroHeptacosanoic acid	76	**519.93g/mol**	$C_{27}H_{32}Cl_2N_2O_4$
61	36.2106	32,880	trans-Traumatic acid	33	228.28g/mol	$C_{12}H_{20}O_4$
62	36.6918	962,800	11-Hexadecenoic acid, 15-methyl-, methyl ester	35	282.5g/mol	$C_{18}H_{34}O_2$
63	36.7348	183,800	Z-6-Pentadecen-1-ol acetate	43	268.4g/mol	$C_{17}H_{32}O_2$
64	36.7647	633,410	1H-Pyrrole-2,4-dicarboxylic acid, 5-formyl-3-methyl-,diethyl ester	56	253.251g/mol	$C_{12}H_{15}NO_5$

Table 9: Showing GC-MS fragments of Sample S [$Mn(HAP)_2.Cl_2$]; molecular ion of [$Mn(HAP)_2.Cl_2$] = 553.93g/mol.

S/N	RT	Area (Pct)	Name of Compound	*m/z*	Mol. Weight	Mol. Formula
1	5.9896	260,710	2-Dodecanol	47	186.33g/mol	$C_{12}H_{26}O$
2	7.05	228,930	Carbazic acid, 3-(1-propylbutylidene)-, ethyl ester	38	200.28g/mol	$C_{10}H_{20}N_2O_2$
3	7.5708	179,630	2-Amino-1-(o-methoxyphenyl)propane	38	181.23g/mol	$C_{10}H_{15}NO_2$
4	7.6106	48,250	Diglycolamine	50	105.1356g/mol	$C_4H_{11}NO_2$
5	8.3262	118,000	Diglycolamine	53	105.1356g/mol	$C_4H_{11}NO_2$
6	8.3433	96,350	N,N-Dimethylethanesulfonamide	53	137.20g/mol	$C_4H_{11}NO_2S$
7	8.9932	143,570	Acetic acid, cyano-	43	85.06g/mol	$C_3H_3NO_2$
8	9.0098	73,420	1,2,4-Triazole, 4-[N-(2-hydroxyethyl)-N-nitro]amino-	53	173.13g/mol	$C_4H_7N_5O_3$
9	9.5145	76,520	2-Amino-4-dimethylaminomethylenepentanedinitrile	38	126.20g/mol	$C_7H_{14}N_2$
10	9.5385	88,120	2-Propenoic acid, 3-(dimethylamino)-3-[(1-methylethy) amino]-, methyl ester	38	158.19826 g/mol	$C_7H_{14}N_2O_2$
11	10.5859	70,550	Azetidin-2-one 3,3-dimethyl-4-(1-aminoethyl)-	40	142.20g/mol	$C_7H_{14}N_2O$
12	10.63	46,710	Acetic acid, (2-propenylthio)-	64	132.181g/mol	$C_5H_8O_2S$
13	12.6543	-11,440	3-Pentanone, dimethylhydrazone	38	128.22g/mol	$C_7H_{16}N_2$
14	13.6428	153,100	Pterin-6-carboxtlic acid	68	207.15g/mol	$C_7H_5N_5O_3$
15	13.7009	37,060	Hexadecanal	47	240.42g/mol	$C_{16}H_{32}O$
16	14.6248	100,470	Piperidine, 3-(bromomethyl)-	43	178.07g/mol	$C_6H_{12}BrN$
17	14.6416	72,140	1-Propanamine, N-nitro-	40	104.11g/mol	$C_3H_8N_2O_2$
18	15.4198	57,370	Z-1,9-Hexadecadiene	27	222.41g/mol	$C_{16}H_{30}$
19	15.4669	92,800	2-(Oxan-3-yl)ethanamine	59	129.20000g/mol	$C_7H_{15}NO$
20	16.5304	77,300	2-(Oxan-3-yl)ethanamine	43	129.20000g/mol	$C_7H_{15}NO$
21	16.5721	39,210	N<2>, N<2>, N<2>, N<2>-Tetramethyl-4,6-bis (trifluoromethyl)-1, 3,5,2.lambda.<5>-triazaph	53		
22	20.3348	31,630	Butylated Hydroxytoluene	98	220.35g/mol	$C_{15}H_{24}O$
23	20.7727	102,040	Methanesulfonamide, N,N-dimethyl-	47	123.174g/mol	$C_3H_9NO_2S$
24	20.7889	75,910	Metaraminol	50	167.20g/mol	$C_9H_{13}NO_2$
25	22.4186	5,330	Butanal, 3-hydroxy-	50	88.1051g/mol	$C_4H_8O_2$
26	24.1953	1,090	Aziridine, 2-(1,1-dimethylethyl)-3-methyl-1-(2-propenyl)-,trans-	47	113.20g/mol	$C_7H_{15}N$
27	25.9879	87,920	Pterin-6-carboxylic acid	58	207.15g/mol	$C_7H_5N_5O_3$
28	28.4692	70,790	4-Carboxy-2,2,5,5-tetramethyl-3-imidazoline[3-N]-1-oxyl	47	201.20000g/mol	$C_8H_{13}N_2O_4$
29	29.2479	19,340	Hexadecanoic acid, methyl ester	94	270.4507g/mol	$C_{17}H_{34}O_2$
30	30.0062	104,490	Hexadecanoic acid, ethyl ester	95	284.4772g/mol	$C_{18}H_{36}O_2$
31	30.8917	23,320	9,12-Octadecanoic acid, methyl ester, (E,E)-	99	294.4721g/mol	$C_{19}H_{34}O_2$
32	30.9347	58,670	9-Octadecenoic acid (Z)-, methyl ester	99	296.4879g/mol	$C_{19}H_{36}O_2$
33	31.4099	581,950	Ethyl Oleate	91	310.5g/mol	$C_{20}H_{38}O_2$
34	31.5804	401,410	Octadecanoic acid, ethyl ester	97	312.5304g/mol	$C_{20}H_{40}O_2$
35	31.6455	27,980	1-Heptadecene	59	238.5g/mol	$C_{17}H_{34}$
36	31.7385	231,860	Oleic acid	78	282.5g/mol	$C_{18}H_{34}O_2$
37	31.7965	216,280	Octadec-9-enoic acid	93	282.5g/mol	$C_{18}H_{34}O_2$
38	31.8258	449,080	Oleic acid	89	282.5g/mol	$C_{18}H_{34}O_2$
39	32.7142	17,660	Ethyl 9-hexadecenoate	45	282.4614g/mol	$C_{18}H_{34}O_2$
40	33.2191	70,860	E-11-Tetradecenoic acid	49	226.3550g/mol	$C_{14}H_{26}O_2$
41	33.2191	85,130	n-Propyl 11-octadecenoate	90	324.5g/mol	$C_{21}H_{40}O_2$
42	33.3233	44,020	9-Octadecenoic acid (Z)-, 2,3-dihydroxypropyl ester	56	356.5399g/mol	$C_{21}H_{40}O_4$
43	33.4935	166,440	Oleic acid	55	282.5g/mol	$C_{18}H_{34}O_2$

44	33.5354	63,450	Oleic acid	41	282.5g/mol	$C_{18}H_{34}O_2$
45	33.6725	240,350	Oleic acid	30	282.5g/mol	$C_{18}H_{34}O_2$
46	33.8096	176,900	2,4-diaminodichloroNonacosanoic acid	79	**553.93g/mol**	$C_{29}H_{42}Cl_2N_2O_4$
47	33.7036	64,720	Hexadecane, 1-(ethenyloxy)-	46	268.485g/mol	$C_{18}H_{36}O$
48	33.8799	694,690	9-Eicosene, (E)-	91	280.5316g/mol	$C_{20}H_4$
49	34.1357	1,214,850	Cyclohexane, 1,1'-(2-propyl-1,3-propanediyl)bis-	38	250.4626g/mol	$C_{18}H_{34}$
50	34.1615	287,910	Oleic acid	38	282.5g/mol	$C_{18}H_{34}O_2$
51	34.1917	746,720	Butyl 9-octadecenoate or 9-18:1	60	338.6g/mol	$C_{22}H_{42}O_2$
52	36.4692	14,540	1-Heptadecanamine	46	255.4824g/mol	$C_{17}H_{37}N$
53	36.8103	780	Z-8-Pentadecen-1-ol acetate	51	268.4g/mol	$C_{17}H_{32}O_2$
54	37.2964	1,023,750	Anthracene, 9,10-dihydro-9,9,10-trimethyl-	27	222.32g/mol	$C_{17}H_{18}$
55	37.3337	112,560	1H-Indole, 5-methyl-2-phenyl-	30	207.27g/mol	$C_{15}H_{13}N$
56	37.357	613,710	Z-8-Pentadecen-1-ol acetate	50	268.4g/mol	$C_{17}H_{32}O_2$

Table 10: Showing GC-MS fragments of Sample T [Mn(PMP+HAP).Cl_2]; molecular ion of [Mn(PMP+HAP).Cl_2] = 536.93g/mol.

S/N	RT	Area (Pct)	Name of Compound	*m/z*	Mol. Weight	Mol. Formula
1	5.8076	251,170	2-Undecanol	32	172.3077g/mol	$C_{11}H_{24}O$
2	5.841	110,900	2-Nonanol	38	144.25g/mol	$C_9H_{20}O$
3	6.697	258,410	Acetic acid, cyano-	47	85.06g/mol	$C_3H_3NO_2$
4	7.583	78,590	Benzaldehyde, 2 hydroxy-	97	122.1213g/mol	$C_7H_6O_2$
5	7.9454	245,970	2-(Oxan-3-yl)ethanamine	27	129.20000g/mol	$C_7H_{15}NO$
6	10.128	151,360	N,N-Dimethylethanesulfonamide	64	137.20g/mol	$C_4H_{11}NO_2S$
7	11.2406	111,100	Acetic acid, cyano-	50	85.06g/mol	$C_3H_3NO_2$
8	11.284	57,030	Propanenitrile, 3-amino-2,3-di(hydroxymino)-	43	128g/mol	$C_3H_4N_4O_2$
9	12.3574	78,200	N<2>, N<2>, N<2>, N<2>-Tetramethyl-4,6-bis(trifluoromethyl)-1,3,5,2.lambda.<5>-triazaphosphinine-2,2-diamine	45		
10	12.3839	32,800	N<2>, N<2>, N<2>, N<2>-Tetramethyl-4,6-bis(trifluoromethyl)-1,3,5,2.lambda.<5>-triazaphosphinine-2,2-diamine	43		
11	12.4083	67,550	Benzaldehyde, 2-nitro-, diaminomethylidenhydrazone	25	207.18936g/mol	$C_8H_9N_5O_2$
12	13.0289	165,490	5-Bromo-N, N-dimethyl-2H-1,2,4-triazole-3-carboxamide	38	219.03900g/mol	$C_5H_7BrN_4O$
13	13.0867	33,780	Pterin-6-carboxylic acid	53	207.15g/mol	$C_7H_5N_5O_3$
14	13.8686	73,300	Azetidin-2-one 3,3-dimethyl-4-(1-aminoethyl)-	58	142.20g/mol	$C_7H_{14}N_2O$
15	13.8918	20,340	Imidazole, 2-amino-5-[(2-carboxy)vinyl]-	43	153.14g/mol	$C_6H_7N_3O_2$
16	13.9393	86,090	Benzoic acid, 2-hydroxy-, ethyl ester	35	166.1739g/mol	$C_9H_{10}O_3$
17	14.6289	-39,660	2-Piperidinone, 1-methyl-	52	113.1576g/mol	$C_6H_{11}NO$
18	14.7032	5,450	2-Amino-4-dimethylaminomethylenepentanedinitrile	37	126.20g/mol	$C_7H_{14}N_2$
19	18.0382	90,580	1,1,1-Trichloro-2-hydroxy-2-[acetamidoethylthio]ethane	45		
20	18.0572	86,120	Methanesulfonamide, N,N-dimethyl	49	123.18g/mol	$C_3H_9NO_2S$
21	19.9585	21,680	Pterin-6-carboxylic acid	58	207.15g/mol	$C_7H_5N_5O_3$
22	20.0063	5,630	1-[.alpha.-(1-Adamantyl)benzylidene]thiosemicarbazide	53	313.5g/mol	$C_{18}H_{23}N_3S$
23	21.1779	3,240	5-Aminoisoxazole	46	84.08g/mol	$C_3H_4N_2O$
24	25.3746	-580	Urea, N-ethyl-N-nitroso-	45	117.1066g/mol	$C_3H_7N_3O_2$
25	27.7098	-14,290	S-[Tri-t-butoxysilyl]-2-mercaptoethylamine	50	323.57g/mol	$C_{14}H_{33}NO_3SSi$
26	29.2635	84,590	Hexadecanoic acid, methyl ester	97	270.4507g/mol	$C_{17}H_{34}O_2$
27	29.7714	78,960	1,2-Benzenedicarboxylic acid, butyl 2-ethylhexyl ester	72	334.4498g/mol	$C_{20}H_{30}O_4$
28	30.0212	1,284,700	Hexadecanoic acid, ethyl ester	98	284.4772g/mol	$C_{18}H_{36}O_2$
29	30.1878	84,610	Oleic acid	70	282.5g/mol	$C_{18}H_{34}O_2$

30	30.2249	202,880	Z-(13,14-Epoxy)tetradic-11-en-1-ol acetate	53	268.39g/mol	$C_{16}H_{28}O_3$
31	30.9033	38,930	9,12-Octadecadienoic acid (Z,Z)-, methyl ester	99	294.4721g/mol	$C_{19}H_{34}O_2$
32	30.9451	99,250	6-Octadecenoic acid, methyl ester, (Z)-	99	296.4879g/mol	$C_{19}H_{36}O_2$
33	31.4196	445,210	Ethyl Oleate	99	310.5g/mol	$C_{20}H_{38}O_2$
34	31.5882	138,700	Octadecanoic acid, ethyl ester	98	312.5304g/mol	$C_{20}H_{40}O_2$
35	32.0217	-620	1-Cyclohexylnonene	64	208.38g/mol	$C_{15}H_{28}$
36	32.7223	27,900	Butanoic acid, 2-methyl-, methyl ester	46	116.1583g/mol	$C_6H_{12}O_2$
37	33.0372	12,230	9-Octadecenoic acid (Z)-, 2,3-dihydroxypropyl ester	27	356.5399g/mol	$C_{21}H_{40}O_4$
38	33.2708	58,130	Z-8-Pentadecen-1-ol acetate	64	268.4g/mol	$C_{17}H_{32}O_2$
39	33.6844	1,354,530	10-Undecenehydroxamic acid	30	216.27g/mol	$C_{11}H_{20}O_4$
40	33.7442	503,680	1-Docosanethiol	59	202.40g/mol	$C_{12}H_{26}S$
41	36.792	2,266,300	9-Octadecenoic acid (Z)-, 2,3-dihydroxypropyl ester	38	356.5399g/mol	$C_{21}H_{40}O_4$
42	36.8294	1,348,770	9-Octadecenoic acid (Z)-, 2,3-dihydroxypropyl ester	90	356.5399g/mol	$C_{21}H_{40}O_4$
43	36.8668	917,530	4,4-diaminodichlorooctacosanoic acid	72	**536.93g/mol**	$C_{28}H_{37}Cl_2N_2O_4$

3.4 FT-IR Spectra

Table 11: Showing the FTIR spectrum data for the ligand 2-phenyliminomethylphenol (PMP) of the characteristics infrared absorption frequencies (Anumata *et al.*, 2024).

Assignment of Bond	Frequency Range in cm^{-1}	Functional Group Type
vC=N stretching	1569.2	Aromatic Amines
C-H bending	1613.9	Aromatic Amines
C-H bending	1833.3	Aromatic ring
C-H bending	1919.6	Aromatic ring
vC=N stretching	2109.7	Aromatic Amines
vC-H stretching	2653.9	Aromatic ring
vC-H stretching	2713.5	Aromatic ring
vC-H stretching	2851.4	Aromatic ring
vC-H stretching	2991.9	Aromatic ring
vC-H vibrations in ring	3056.4	Aromatic ring
vO-H	3213.0	Phenolic
vO-H	3652.8	Phenolic

Table 12: Showing the FTIR spectrum data for the ligand 2,2-hydroxybenzylideneaminophenol (HAP) of the characteristics infrared absorption frequencies (Anumata *et al.*, 2024).

Assignment of Bond	Frequency Range in cm^{-1}	Functional Group Type
vC-H stretching	1528.2	Aromatic ring
vC-H stretching	1804.8	Aromatic ring
vC-H stretching	1848.0	Aromatic ring
vC-H vibrations in ring	1990.4	Aromatic ring
vC-H stretching	2113.4	Aromatic ring
vC-H stretching	2374.3	Aromatic ring
vC-H stretching	2542.0	Aromatic ring
vC-H stretching	2691.1	Aromatic ring
vC-H stretching	2851.4	Aromatic ring
vC-H stretching	2926.0	Aromatic ring
vC-H vibrations in ring	3045.2	Aromatic ring
vO-H	3634.2	Phenolic
vO-H	3678.9	Phenolic

Table 13: FTIR spectral data for 2-phenyliminomethylphenol Iron(II) chloride complex showing the characteristics infrared absorption frequencies.

Assignment of bond	Frequency Range in cm^{-1}	Functional group type
C=N bending	1606.5	Aromatic Amines
vC-H stretching	1994.1	Aromatic Ring
vC=N stretching	2117.1	Aromatic Amines
vO-H	3186.9	Phenolic
vO-H	3589.4	Phenolic

Table 14: FTIR spectral data for 2,2-hydroxybenzylideneaminophenol Iron(II) chloride complex showing the characteristics infrared absorption frequencies.

Assignment of bond	Frequency Range in cm^{-1}	Functional group type
vC=C stretching	1632.6	Aromatic Ring
vC-H stretching	1811.5	Aromatic Ring
vC-H stretching	1994.1	Aromatic Ring
vC=N stretching	2113.4	Aromatic Amines
vO-H stretching	3339.7	Phenolic

Table 15: FTIR spectral data for mixed ligand (PMP+HAP) Iron(II) chloride complex showing the characteristics infrared absorption frequencies.

Assignment on bond	Frequency Range in cm^{-1}	Functional group type
vC-H stretching	1602.8	Aromatic Ring
vC-H stretching	1636.3	Aromatic Ring
vC-H stretching	1804.0	Aromatic Ring
vC-H stretching	1990.4	Aromatic Ring
vC=N stretching	2102.2	Aromatic Amines
vC=N stretching	2553.2	Aromatic Amines
vO-H	3052.7	Phenolic

Table 16: FTIR spectral data for 2-Phenyliminomethylphenol Manganese(II) chloride complex showing the characteristics infrared absorption frequencies.

Assignment of Bond	Frequency Range in cm^{-1}	Functional Group Type
vC=C stretching	1613.9	Phenolic
vC=C stretching	1654.9	Aromatic Ring
vC=C stretching	1736.9	Aromatic Ring
vC-H stretching	1796.6	Aromatic Ring
vC-H stretching	1882.3	Aromatic Alkene
vC-H stretching	1949.4	Aromatic Alkene
vC=N stretching	2109.7	Aromatic Amines
vC=N stretching	2370.6	Aromatic Amines
vC=N stretching	2653.9	Aromatic Amines
vO-H	3339.7	Phenolic
vO-H	3652.8	Phenolic
vO-H	3712.4	Phenolic
vO-H	3753.4	Phenolic

Table 17: FTIR spectral data for 2,2-hydroxybenzylideneaminophenol Manganese(II) chloride complex showing the characteristics infrared absorption frequencies.

Assignment of Bond	Frequency Range in cm^{-1}	Functional Group Type
vC=C stretching	1606.5	Aromatic Ring
vC-H streching	1927.0	Aromatic Alkene
vC=N stretching	2113.4	Aromatic Amines
vO-H	3339.7	Phenolic
vO-H	3712.4	Phenolic

Table 18: FTIR spectral data for mixed ligand (PMP+HAP) Manganese(II) chloride complex showing the characteristics infrared absorption frequencies.

Assignment of Bond	Frequency Range in cm^{-1}	Functional Group Type
vC=C stretching	1572.9	Aromatic Ring
vC-H stretching	1922.9	Aromatic Ring
vC=N stretching	2117.4	Aromatic Amines
vC=N stretching	2376.6	Aromatic Amines
vO-H	3324.4	Phenolic
vO-H	3712.4	Phenolic
vO-H	3753.4	Phenolic

The FTIR spectral interpretations/data are given in Tables 13, 14 and 15 respectively, while the infrared spectra of FTIR spectra for 2-phenyliminomethylphenol Iron(II) Chloride complex $[Fe(PMP)_2.Cl_2]$, 2,2-hydroxybenzylideneaminophenol Iron(II) Chloride complex $[Fe(HAP)_2.Cl_2]$ and mixed ligand of PMP and HAP of Iron(II) Chloride$[Fe(PMP+HAP).Cl_2]$ are presented in Appendix E (c–e). The spectra for the metal complexes were compared with that of the original ligand PMP and HAP as shown in Appendix E (a–b). The original ligand and complexes showed dissimilarity in their spectra suggesting the bonding of Fe^{2+} with PMP and HAP and Cl^-. For $[Fe(PMP)_2.Cl_2]$, C=N bending were noticed at 1606.5cm^{-1} bands vC-H srtetching vibrations in Benzene rings were at bands of 1994.1cm^{-1}, vC=N stretching were observed at bands of 2117.1 cm^{-1} and vO-H stretching were found at 3186.9 cm^{-1} and 3589.9 cm^{-1} bands respectively. For $[Fe(HAP)_2.Cl_2]$, C=O The vC=C stretching were found at 1539.4 cm^{-1} and 1652.6 cm^{-1} bands while vC-H stretching were at bands 1811.5 cm^{-1} and 1994.1 cm^{-1} respectively, and vO-H stretching were between 3339.7 cm^{-1}. For the mixed ligands of $[Fe(PMP+HAP).Cl_2]$, vC=C stretching were found at 1539.4 cm^{-1} bands, vC-H stretching were at 1602.8 cm^{-1} – 1990.4 cm^{-1}, vC=N stretching of the aromatic rings observed at 2105.2 cm^{-1} and 2553.2 cm^{-1} bands respectively. The broad absorption band at the 3339.7 cm^{-1} for the mixed Fe^{2+} which were present in the spectra of the metal complexes of Fe^{2+} was assigned to vOH of the enol form of the ligand (Chris & John, 2007). However, the broad band appearing in the 3589.4 cm^{-1} of the FTIR spectra region for Fe^{2+} complexes have been attributed to vOH of adduct of water molecules coordinated to the central metal ion or residing in the crystal lattices of the complexes (Ogwuegbu *et. al.*, 2019). Furthermore, the absorption band at 2553.2 cm^{-1} due to C=N vibration in the spectrum of 2-phenyliminomethylphenol was shifted in the spectra of the prepared complex. This shows that the coordination of $[Fe(PMP)_2.Cl_2]$ is between N of the C=N (imine) group and the metal of the complex.

The infrared spectra of FTIR spectra for 2-phenyliminomethylphenol Manganese(II) Chloride complex $[Mn(PMP)_2.Cl_2]$, 2,2-hydroxybenzylideneaminophenol Manganese(II) Chloride complex $[Mn(HAP)_2.Cl_2]$ and mixed ligand of PMP and HAP of Manganese(II) Chloride $[Mn(PMP+HAP).Cl_2]$ are presented in Appendix E (f–h) and the spectral interpretation/data given in Tables 16, 17 and 18 respectively. The spectra for the metal complexes were compared with that of the original ligand PMP and HAP shown in Appendix E (a–b). The original ligand and complexes showed dissimilarity in their spectra suggesting the bonding of Mn^{2+} with PMP and HAP and Cl^-. For $[Mn(PMP)_2.Cl_2]$, vC=C stretching were at 1613.9cm^{-1} bands while vC-H stretching were at 1796.6cm^{-1} -1949.4cm^{-1}, vC=N stretching were observed at bands of 2109.7 cm^{-1}, 2370.6 cm^{-1} and 2653.9 cm^{-1} respectively and vO-H stretching were found at 3339.7 cm^{-1} – 3753.4 cm^{-1} bands. For $[Mn(HAP)_2.Cl_2]$, The vC=C stretching were found at 1606.5 cm^{-1} bands, the vC-H stretching were at 1927.0 cm^{-1} bands while vC=N stretching were at bands 2113.4 cm^{-1}, and vO-H stretching were at 3339.7 cm^{-1} and 3712.4 cm^{-1}. For the mixed ligands of $[Mn(PMP+HAP).Cl_2]$, vC=C stretching were found at 1572.9 cm^{-1} bands, vC=N stretching of the aromatic rings observed at 2117.4 cm^{-1} and 2376.6

cm^{-1} bands respectively and vO-H stretching were noticed at 3324.4 cm^{-1} to 3753.4 cm^{-1} bands. The broad absorption band at the 3753.4 cm^{-1} for the mixed Mn^{2+} which were present in the spectra of the metal complexes of Mn^{2+} was assigned to vOH of the enol form of the ligand (Chris & John, 2007). However, the broad band appearing in the 3583.3 cm^{-1} of the FTIR spectra region for Mn^{2+} complexes have been attributed to vOH of adduct of water molecules coordinated to the central metal ion or residing in the crystal lattices of the complexes (Ogwuegbu *et. al.,* 2019). Furthermore, the absorption band at 2376.6 cm^{-1} due to C=N vibration in the spectrum of 2-phenyliminomethylphenol was shifted in the spectra of the prepared complex. This shows that the coordination of $[Mn(PMP)_2.Cl_2]$ is between N of the C=N (imine) group and the metal of the complex.

3.5 UV-Vis Spectra

The electronic spectra of the complexes formed are presented in Appendix F (a–f) while the spectral data were listed in Table 19. The energy absorbed from the ultraviolet/visible radiation causes changes in the electronic energy of the compound resulting from transition of valence electrons in the complexes (Anumata *et al.,* 2024). These electronic transitions consist of the excitation of an electron from an occupied molecular orbital, typically a non-bonding (n) or a bonding (π) to an unoccupied molecular orbital, *i.e.* $n \rightarrow \pi^*$ or $\pi \rightarrow \pi^*$ respectively. However, it is not all electronic transitions that are permitted (Waheb & Adedibu, 2003; Ogwuegbu *et al.*, 2019).

Table 19: UV-Visible spectra for mixed ligand Iron(II) chloride and Manganese(II) chloride complexes.

Compounds	Wavelength (nm)	Elemental transition
$[Fe(PMP)_2.Cl_2]$	312	$\pi \rightarrow \pi^*$
$[Fe(HAP)_2.Cl_2]$	349	$\pi \rightarrow \pi^*$
$[Fe(PMP+HAP).Cl_2]$	417	$\pi \rightarrow \pi^*$
$[Mn(PMP)_2.Cl_2]$	369	$\pi \rightarrow \pi^*$
$[Mn(HAP).Cl_2]$	428	$\pi \rightarrow \pi^*$
$[Mn(PMP+HAP).Cl_2]$	286	$\pi \rightarrow \pi^*$

The UV-Vis spectrum of the complexes were characterized mainly by one absorption and thus appear to have virtually identical spectra, and absorb in the near visible region around λ_1=312nm, 349nm, 417nm, 369nm, 428nm and 286nm for $[Fe(PMP)_2.Cl_2]$, $[Fe(HAP)_2.Cl_2]$, $[Fe(PMP+HAP)_2.Cl_2]$, $[Mn(PMP)_2.Cl_2]$, $[Mn(HAP)_2.Cl_2]$ and $[Mn(PMP+HAP).Cl_2]$ complexes. These absorptions are ascribed to $\pi \rightarrow \pi^*$. The close absorption spectra of the ligand and the metal complexes suggest that the π -bonding system of the free nitro group is intact in the ligand of the metal complexes (Ogwuegbu & Maseka, 1998), indicating that there are no interaction between the metal ions and π-bonding system of the ligand. The coordination between the ligand and the metal ions is therefore through bond formation between the metal ions and the O atom of the hydroxyl group of the ligand.

3.6 XRD Findings

The XRD spectral (powder study) for the different synthesized ligands PMP and HAP and Fe^{2+} and Mn^{2+} complexes are presented in Appendix G (a–f) and the spectral interpretation given in Tables 20–27.

Table 20: FWHM values, average crystallite sizes calculated using Scherrer's formula, D-spacing, and Bragg's diffraction degree of 2-PMP ligand synthesized (Anumata *et al.*, 2024).

Bragg's diffraction [°2Θ]	Full width at half maximum (FWHM) (degrees)	d-spacing [Å]
PMP		
9.8808	0.1574	8.95195
11.7117	0.1574	7.55628

12.4831	0.1968	7.09100
12.9439	0.1378	6.83958
13.8742	0.4723	6.38301
15.4647	0.1378	5.72993
16.7218	0.2362	5.30191
17.1345	0.1181	5.17511
18.4386	0.1181	4.81192
18.8751	0.1181	4.70163
19.0686	0.0984	4.65435
21.4763	0.1771	4.13768
23.7810	0.2362	3.74164
25.6052	0.3936	3.47907
27.6052	0.6298	3.23139
28.0226	0.1181	3.18420
28.8981	0.1181	3.08970
29.3573	0.2755	3.04240
30.4013	0.3149	2.94026
34.2139	0.0787	2.62084
38.0036	0.1574	2.36776
38.8284	0.3149	2.31934
39.7807	0.2362	2.26599
44.2773	0.1968	2.04574
48.1090	0.4723	1.89138
49.9102	0.3936	1.82726
64.4521	0.3149	1.44570
Average crystallite size = 459.09 nm		

Table 21: FWHM values, average crystallite sizes calculated using Scherrer's formula, d-spacing, and Bragg's diffraction degree of 2,2-HAP ligand synthesized (Anumata *et al.*, 2024).

Bragg's diffraction [°2Ɵ]	Full width at half maximum (FWHM) (degrees)	d-spacing [Å]
HAP		
8.5287	0.4723	10.36788
9.3516	0.0984	9.45732
9.6897	0.2362	9.12802
13.2924	0.1378	6.66104
13.6907	0.2755	6.46813
14.7029	0.1181	6.02507
15.1847	0.1771	5.83495
15.3412	0.1181	5.77577
19.3409	0.4723	4.58943
20.8612	0.6298	4.25827
22.5581	0.9446	3.94164
24.3965	0.1181	3.64864
27.2967	0.1574	3.26721
34.2415	0.1181	2.61879
35.5234	0.6298	2.52717
38.0154	0.1968	2.36705
39.7603	0.1181	2.26710
44.2581	0.0787	2.04659
45.8873	0.4723	1.97764
49.5299	0.2362	1.84040
64.4553	0.1181	1.44564
68.8234	0.2362	1.36416
Average crystallite size = 473.52 nm		

Table 22: FWHM values, average crystallite sizes calculated using Scherrer's formula, d-spacing, and Bragg's diffraction degree of 2-PMP iron(II) chloride complex synthesized.

Bragg's diffraction [°2Θ]	Full width at half maximum (FWHM) (degrees)	d-spacing [Å]
[$Fe(PMP)_2$. Cl_2]		
7.9081	0.1574	11.18001
29.1068	0.4723	3.06801
38.0330	0.1968	2.36600
Average crystallite size = 368.89 nm		

Table 23: FWHM values, average crystallite sizes calculated using Scherrer's formula, d-spacing, and Bragg's diffraction degree of 2,2-HAP iron(II) chloride complex synthesized.

Bragg's diffraction [°2Θ]	Full width at half maximum (FWHM) (degrees)	d-spacing [Å]
[$Fe(HAP)_2.Cl_2$]		
10.2236	0.4723	8.65256
18.3028	0.9446	4.84733
26.3041	0.7872	3.38819
Average crystallite size = 119.23 nm		

Table 24: FWHM values, average crystallite sizes calculated using Scherrer's formula, d-spacing, and Bragg's diffraction degree of mixed ligand (2-PMP+2,2-HAP) iron(II) chloride complex synthesized.

Bragg's diffraction [°2Θ]	Full width at half maximum (FWHM) (degrees)	d-spacing [Å]
[$Fe(PMP+HAP)_2.Cl_2$]		
11.0221	0.1786	8.11201
27.9460	0.4935	5.43401
36.9662	0.2755	2.70201
Average crystallite size = 249.66		

Table 25: FWHM values, average crystallite sizes calculated using Scherrer's formula, d-spacing, and Bragg's diffraction degree of 2-PMP manganese(II) chloride complex synthesized.

Bragg's diffraction [°2Θ]	Full width at half maximum (FWHM) (degrees)	d-spacing [Å]
[$Mn(PMP)_2.Cl_2$]		
11.495	0.34	7.692
12.699	0.126	6.965
12.914	0.115	6.849
15.33	0.11	5.776
17.072	0.38	5.189
18.599	0.26	4.767
18.824	0.125	4.7105
21.38	0.37	4.153
22.062	0.09	4.0259
23.510	0.111	3.7811
23.755	0.205	3.7426
24.352	0.099	3.6522
25.392	0.14	3.5049
25.681	0.120	3.4660
26.231	0.25	3.395
28.00	0.41	3.184
28.511	0.104	3.1281
29.000	0.139	3.0765
29.31	0.54	3.045
34.151	0.13	2.6234
Average crystallite size = 546.75 nm		

Table 26: FWHM values, average crystallite sizes calculated using Scherrer's formula, d-spacing, and Bragg's diffraction degree of 2,2-HAP manganese(II) chloride complex synthesized.

Bragg's diffraction [°2Θ]	Full width at half maximum (FWHM) (degrees)	d-spacing [Å]
$[Mn(HAP)_2.Cl_2]$		
8.60	0.84	10.27
37.995	0.187	2.3663
44.24	0.19	2.0459
Average crystallite size = 347.67 nm		

Table 27: FWHM values, average crystallite sizes calculated using Scherrer's formula, d-spacing, and Bragg's diffraction degree of mixed ligand (2-PMP+2,2-HAP) manganese(II) chloride complex synthesized.

Bragg's diffraction [°2Θ]	Full width at half maximum (FWHM) (degrees)	d-spacing [Å]
$[Mn(PMP+HAP).Cl_2]$		
11.0221	0.1786	8.11201
27.9460	0.4935	5.43401
36.9662	0.2755	2.70201
Average crystallite size = 249.66 nm		

X-ray diffractograms of the metal complexes investigated showed good intense peaks indicating high crystallinity except for 2-phenylaminomethylphenol manganese(II) complexes with reduced and broadened peak indicating their less crystalline. Similar observation was made for Fe(II) and Mn(II) complexes of 4(4-(dimethylamino) benzylideneamino)benzoic acid (Khan *et al.*, 2013). Crystalline nature of the complexes was indicated by comparing the diffractograms with their respective ligands, see Appendix G (a–b), and results showed marked differences, which indicate complexation have really occurred.

3.7 Antimicrobial Activities of Synthesized Iron and Manganese Complexes

The results obtained from the antimicrobial screening of the ligands PMP and HAP and the metal complexes of Fe^{2+} and Mn^{2+} are presented in Table 28 that follows.

Table 28: Showing inhibitory action of iron and manganese metal complexes across different classes of micro-organisms.

	PMP	HAP	$[Fe(PMP)_2.Cl_2]$	$[Fe(HAP)_2.Cl_2]$	$[Fe(PMP+HAP).Cl_2]$	$[Mn(PMP)_2.Cl_2]$	$[Mn(HAP)_2.Cl_2]$	$[Mn(PMP+HAP)_2.Cl_2]$
Gram positive bacteria								
Staphyloccocus aureus	+	+	+	++	+++	+	++	+++
Bacillus substilis	+	+	++	+++	+++	++	+++	+++
Gram negative bacteria								
Escherichia coli	+	+	++	+	++	+++	+++	+++
Pseudomonas aeruginosa	+	+	++	+++	+++	+	+++	+++
Fungi Pathogenic Species								
Candida albicans	-	-	+	+	++	+	++	+++
Aspergillus niger	-	+	++	++	++	++	+++	+++

Key: - shows no inhibitory action, + shows weak or partial inhibitory action, ++ shows stronger inhibitory action, +++ shows strongest inhibitory action, – shows no inhibition

The complex $[Fe(PMP)_2.Cl_2]$ showed partial inhibitory action on *Staphylococcus* aureus and only strong inhibition on *Bacillus substilis* of Gram Positive bacteria while it showed strong inhibitory action on both *Escherichia coli* and *Pseudomonas aeruginosa* of Gram Negative bacteria, on the fungi specie it showed weak inhibition on *Candida*

aalbicans but only strong inhibition on *Aspergillus niger*. The complex [Fe(HAP)$_2$.Cl$_2$] showed strong inhibitory action on *Staphylococcus aureus* but stronger inhibition on *Bacillus substilis* of Gram Positive bacteria while it only showed weak inhibtion on *Escherichia coli* but stronger inhibition on *Pseudomonas aeruginosa* of Gram Negative bacteria while on fungi species, it showed weak inhibitory action on *Candida albicans* and only strong inhibition on *Aspergillus niger*. The mxed ligand of iron [Fe(PMP+HAP)$_2$.Cl$_2$] showed stronger inhibition on both *Staphylococcus aureus* and *Bacillus substilis* of Gram Positive bacteria but showed only a strong inhibitory action on *Escherichia coli* but a stronger inhibition on *Pseudomonas aeruginosa* of Gram Negative bacteria while the fungi species, it showed only strong inhibition on both *Candida albicans* and *Aspergillus niger*. The complex [Mn(PMP)$_2$.Cl$_2$] showed only partial inhibitory action on *Staphylococcus aureus* and only a strong inhibition on *Bacillus substilis* of Gram Positive bacteria, while it showed stronger inhibition on *Eschherichia coli* and only a weak inhibitory action on *Pseudomonas aeruginosa* of Gram Negative bacteria, on the fungi species it showed only a partial inihibition on *Candida albicans* and strong inhibitory action on *Aspergillus niger*. The complex [Mn(HAP)$_2$.Cl$_2$] showed a strong inhibition on *Staphylococcus aureus* and a stronger inhibition on *Bacillus substilis* of Gram Positive bacteria while it showed stronger inhibition on both *Escherichia coli* and *Pseudomonas aeruginosa* of Gram Negative bacteria, for the fungi species it showed only strong inhibitory action on *Candida albicans* and stronger inhibition on *Aspergillus niger*. The mixed ligand complexes of manganese [Mn(PMP+HAP)$_2$.Cl$_2$] showed stronger inhibition on both *Staphylococcus aureus* and *Bacillus substilis* of Gram Positive, then *Escherichia coli* and *Pseudomonas aeruginosa* of Gram Negative bacteria and on both *Candida albicans* and *Aspergillus niger* of fungi species.

4. CONCLUSION

From the results, the following conclusions can be drawn:

1. The complexes involving 2-phenyliminomethylphenol (PMP) and 2,2-hydroxybenzylideneaminophenol (HAP) i.e [Fe(PMP)$_2$.Cl$_2$], [Mn(PMP)$_2$.Cl$_2$], [Fe(HAP)$_2$.Cl$_2$], [Mn(HAP)$_2$.Cl$_2$], [Fe(PMP+HAP).Cl$_2$], and [Mn(PMP+HAP).Cl$_2$], had been synthesized and the following melting points 94°C, 95°C, 70°C, 68°C, 93°C and 96°C respectively, which were all higher than the ligand (50°C).
2. The increases in melting point are attributed to the increase in mass of the formed complexes and thus provide evidence for complexation. However, for the 2,2-hydroxybenzylideneaminophenol (HAP) with melting point of 106°C, was higher than it formed metal complexes with 70°C, 68°C, 93°C, and 96°C for [Fe(HAP)$_2$.Cl$_2$], [Mn(HAP)$_2$.Cl$_2$], [Fe(PMP+HAP).Cl$_2$] and [Mn(PMP+HAP).Cl$_2$] respectively.
3. All complexes formed as well as their ligands were strongly soluble in Dimethylsulfoxide (DMSO).
4. The Iron (II), and Manganese (II) complexes are found to have octahedral geometry with 2-phenyliminomethylphenol and octahedral with 2,2-hydroxybenzylideneaminophenol distorted-octahedral with the mixed ligands. The ligand behaves as a bidentated ligand coordinated to the metal ions via oxygen atom of carbonyl group and nitrogen atoms of two imine groups for the complexes.
5. The XRD pattern is indicative that the ligand and metal complexes are crystalline in nature with large crystallite size. The ligands 2-phenyliminomethylphenol (PMP) and 2,2-hydroxybenzylideneaminophenol (HAP) showed weak inhibitory action on the clinical isolates of Gram Positive Bacteria, Gram Negative and no inhibiton on Fungi Species while the Fe(II) and Mn(II) complexes showed either strong or stronger inhibition.

5. REFERENCES

1. Ahmad Sabry Abu-Khadra, Rabie Saad Farag, Alaa El-Dine Mokhtar Abdel-Hady (2016) Synthesis, Characterization and Antimicrobial Activity of Schiff Base (E)-N-(4-(2-Hydroxybenzylideneamino) Phenylsulfonyl) Acetamide Metal Complexes. *American Journal of Analytical Chemistry*, 7(3): 233-245, DOI: 10.4236/ajac.2016.73020
2. Anumata, S.E., Ezenweke, L.O. and Orjiaka, E.N. (2024) Synthesis, Characterization and Antimicrobial Analysis of Nickel and Cobalt Complexes of Condensates of Salicylaldehyde and 2-Hydroxy Aniline. *Asian Journal of Chemical Sciences*, 14(4): 67-93, https://doi.org/10.9734/ajocs/2024/v14i4318
3. Anumata, S.E., Ezenweke, L.O. and Orjiako, E.N. (2025) Synthesis, Chemical Analysis and Antimicrobial Studies of Platinum and Copper Complexes of Condensates of Salicylaldehyde and 2-Hydroxyaniline. *European Journal of Biomedical and Pharmaceutical Sciences*, 12(2):1-38
4. Chris, J.J and John, R.T (2007) Medicinal Application of Coordination Chemistry,Royal Society of Chemistry, Burbington House,London,13-87
5. Hartwig J.F. (2010), Organometallic Metal Chemistry, from Bonding to Catalysis, *University Sciences Books:* New York. 1st Edition
6. Khan, M.I., Khan, A., Hussain, I., Khan, M.A., Gul, S. and Iqbal, M. (2013) Spectral, XRD, SEM and Biological Properties of new Mononuclear Schiff base transition Metal Complexes. *Inorganic Chemistry Communications*, 35:104-109, DOI:10,1016j.inoche.2013.016.014
7. Kay S., Walther B., Peter K., G. Kettenbach, Peter Mayer, Dieter Klemm and Saran, D. (2000). Cellulose Solutions in Water Containing Metal Complexes, *Macromolecules*, 33, 4094-4107
8. Lawal, A., Amolegbe, S.A., Rajee, A.O., Babamale, H.F and Yunus-Issa, M.T. (2015) World Applied Science Journal 33(2): 336-342, 2015 ISSN: 1818-4952
9. Miessler, Gary L., Fischer, Paul J., Tarr, Donald A. (2014) Inorganic Chemistry Pearson Publishers 5th Edition
10. Ogwuegbu, M.O.C. and Maseka, K.K. (1998) Studies on the Coordination Complexes of Calcium(II),Cadmium(II), and Titanium(IV) with P-nitrobenzoyl-5-oxopyrazole. *Bulletin Chemical Society of Ethiopia*, 12(1):27-33
11. Ogwuegbu, M.O.C., Enenebeaku, C.K., Obi, C.S., Ebosie, N.P. and Enyoh, C.E. (2019) Stoichiometric Determination of Fe(II), Ni(II),and Cu(II) Complexes of Metronidazole. *International Journal of Chemical Sciences*, 3(1):25-29
12. Reddy P.R, and Rao K.S. (2006). Ternary nickel(II) complexes as hydrolytic DNA-cleavage agents. Chem Biodivers 3(2): 231-244
13. Sherif, E.A.A. and Eldebss, T.M. (2011) Synthesis, spectral characterization, solution equilibria, *In vitro* antibacterial and cytotoxic activities of Cu(II), Ni(II), Mn(II), Co(II) and Zn(II) complexes with Schiff base derived from 5-bromosalicylaldehyde and 2-aminomethylthiophene. *Spectrochimica Acta Part A: Molecular and biomolecular spectroscopy*, 79:1803-1814
14. Waheb, A.O and Adedibu, C.T. (2003) Synthesis and Characterization of some Metal Complexes of Bis(2-Hydroxy-4-methoxyacetophenone)ethylenediamine. *Indian Journal of Chemistry*, 3(1):25-29

Appendices

Appendix A. Suggested Structures

(a) 2-Phenyliminomethylphenol of Iron (II) Complex

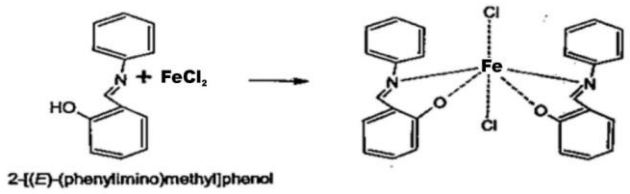

2-[(*E*)-(phenylimino)methyl]phenol

(b) 2,2-Hydroxybenzylideneaminophenol of Iron (II) complex

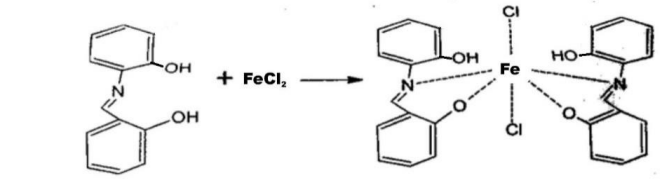

2-{(*E*)-[(3-hydroxyphenyl)imino]methyl}phenol

(c) Mixed ligand (PMP+HAP) of Iron (II) Complex

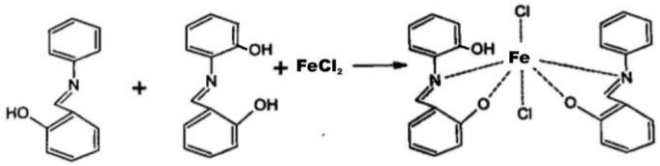

(d) 2-Phenyliminomethylphenol of Manganese (II) Complex

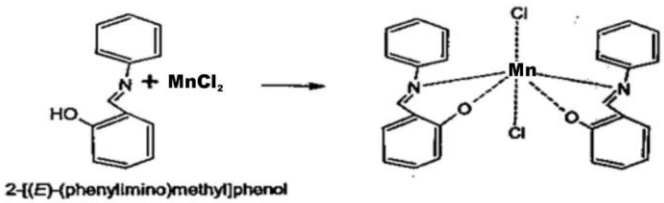

2-[(*E*)-(phenylimino)methyl]phenol

(e) 2,2-Hydroxybenzylideneaminophenol of Manganese (II) complex

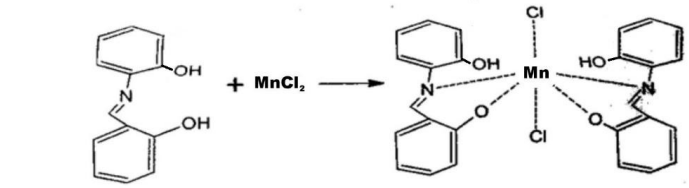

2-{(*E*)-[(3-hydroxyphenyl)imino]methyl}phenol

(f) Mixed ligand (PMP + HAP) of Manganese (II) Complex

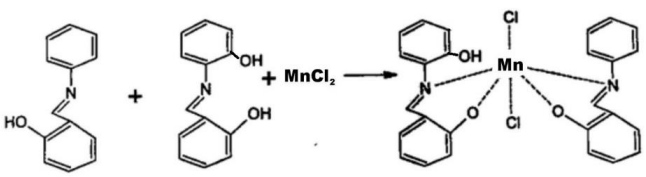

Appendix B. ^{1}HNMR Spectra of the Ligands

(a) ^{1}HNMR Spectra of the Ligand 2-Phenyliminomethylphenol (PMP) (Anumata *et a.*, 2024)

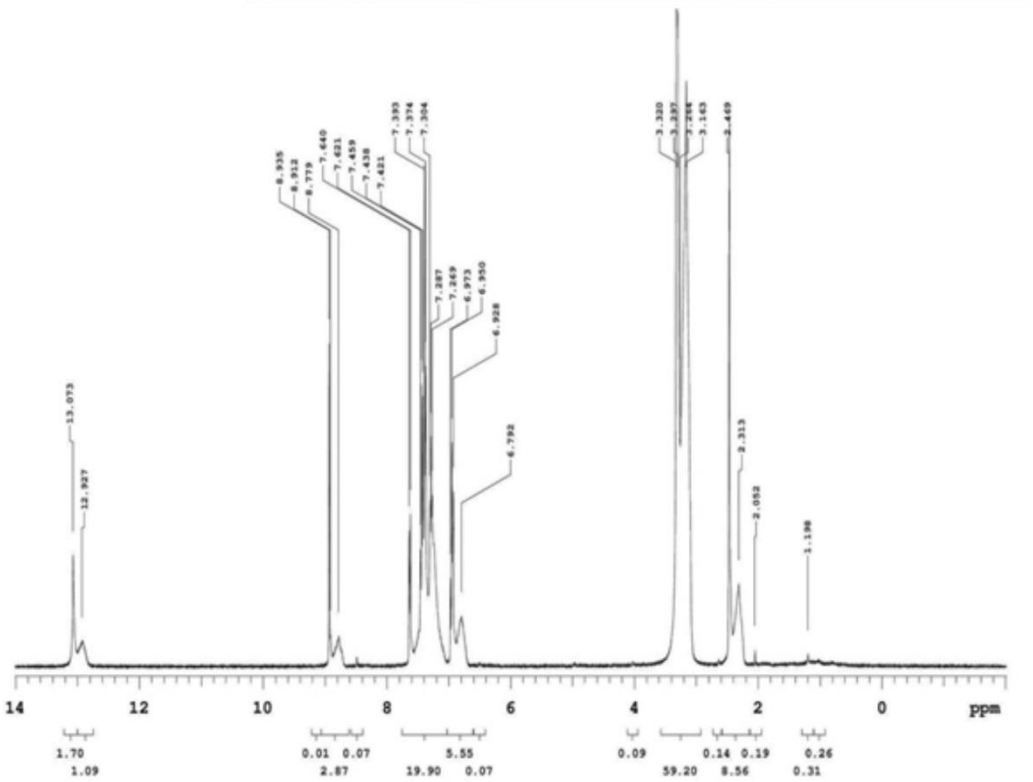

(b) ^{1}HNMR Spectra of the Ligand 2,2 Hydroxybenzylideneaminophenol (HAP) (Anumata *et al.*, 2024)

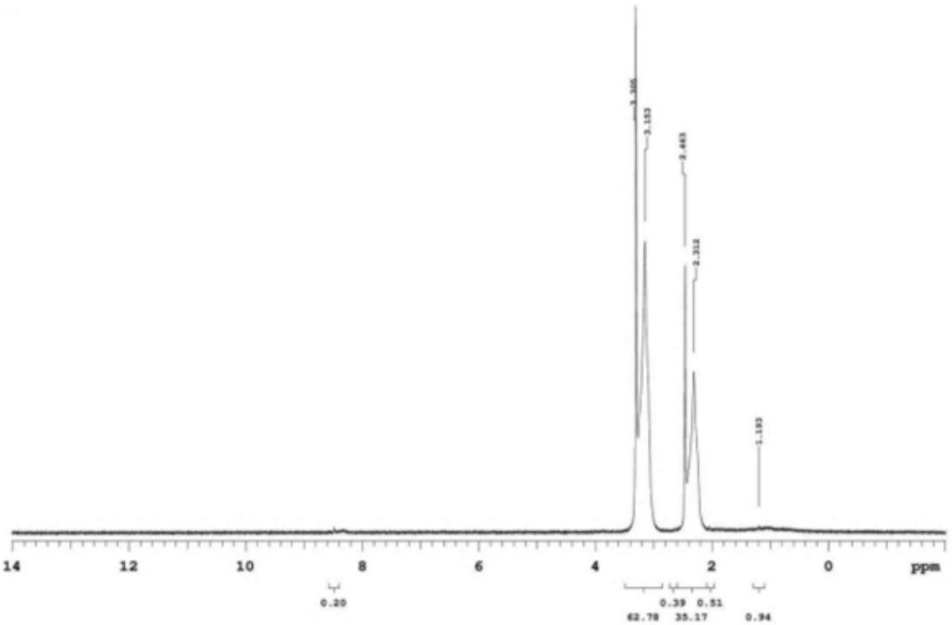

Appendix C. GC-MS Spectra of the Ligands

(a) GC-MS Spectrum of Sample A (2-PMP) (Anumata *et al.*, 2024)

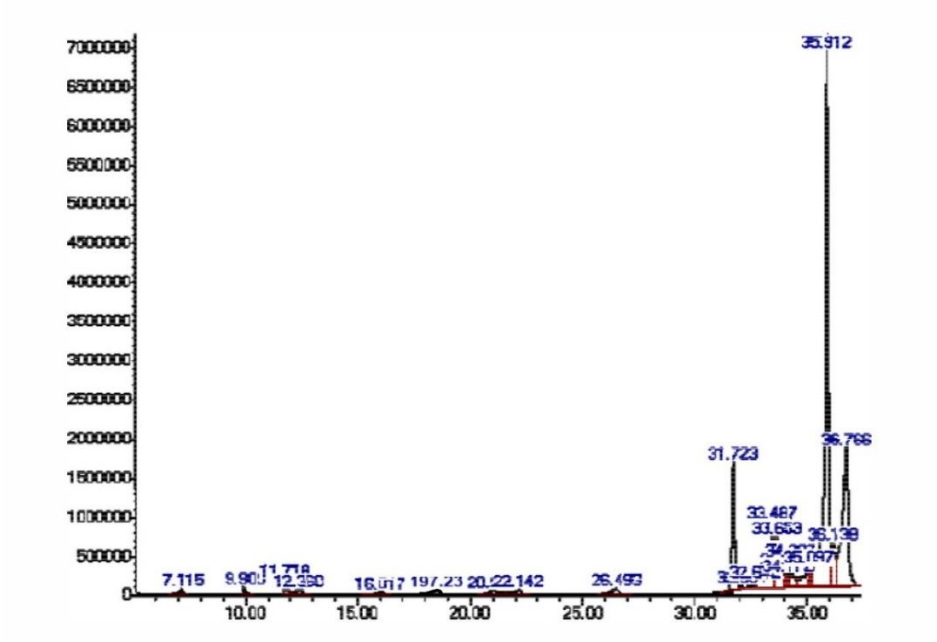

(b) GC-MS Spectrum of Sample B (2,2-HAP) (Anumata *et al.*, 2024)

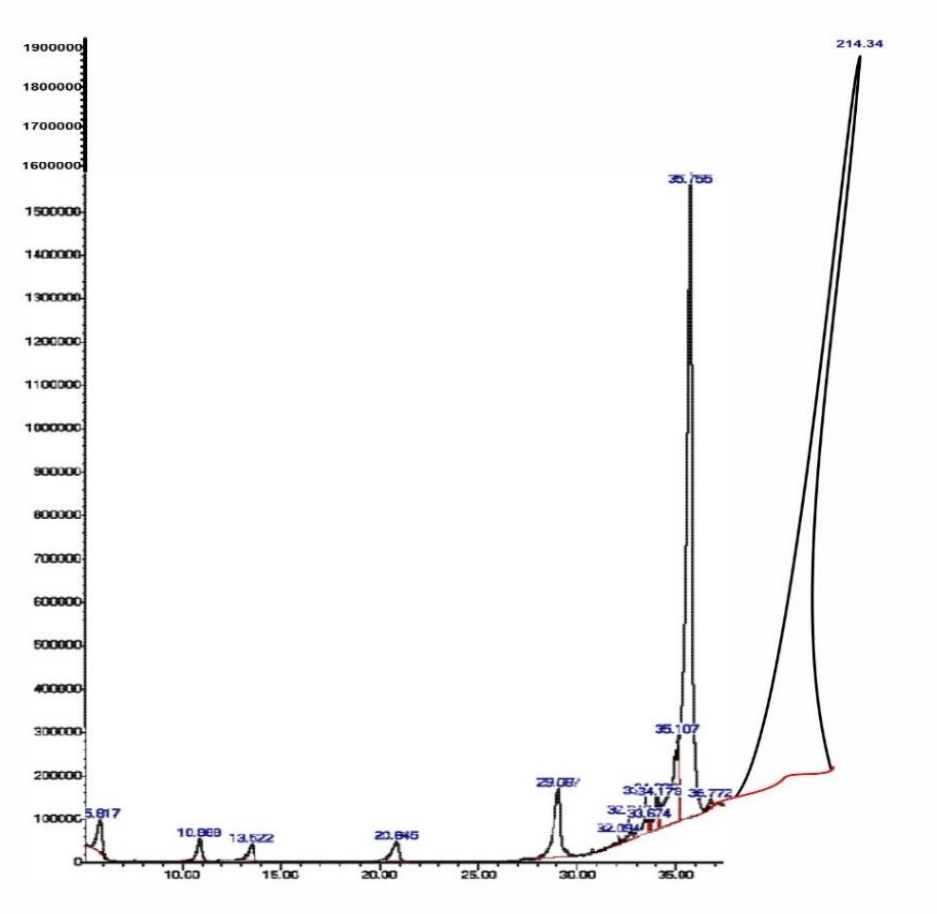

Appendix D. GC-MS Spectra of Samples

(a) GC-MS Spectrum of Sample O [$Fe(PMP)_2.Cl_2$]

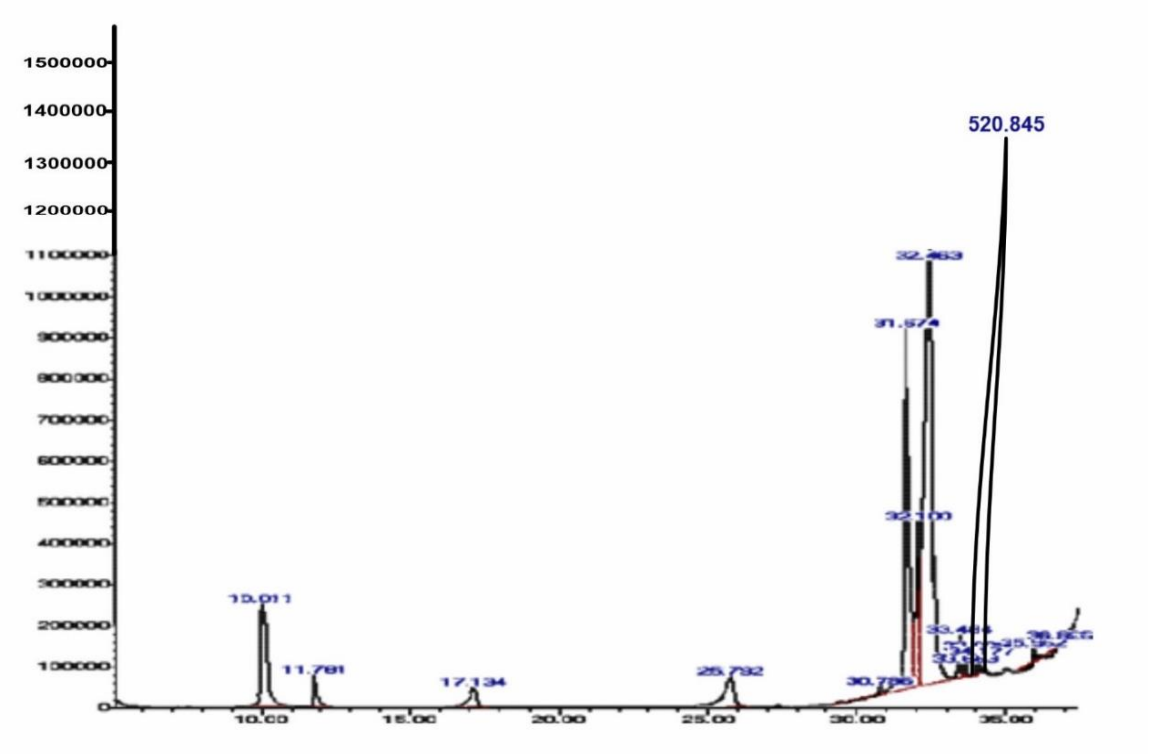

(b) GC-MS Spectrum of Sample P [$Fe(HAP)_2.Cl_2$]

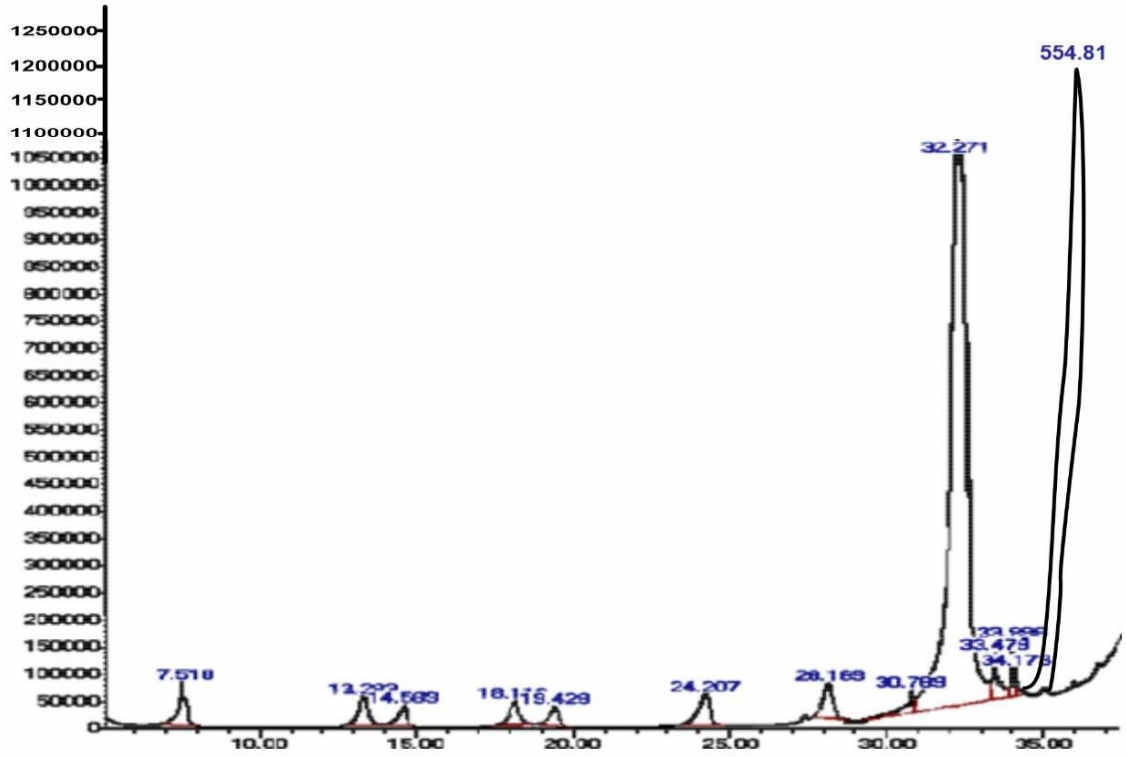

(c) GC-MS Spectrum of Sample Q [$Fe(PMP+HAP).Cl_2$]

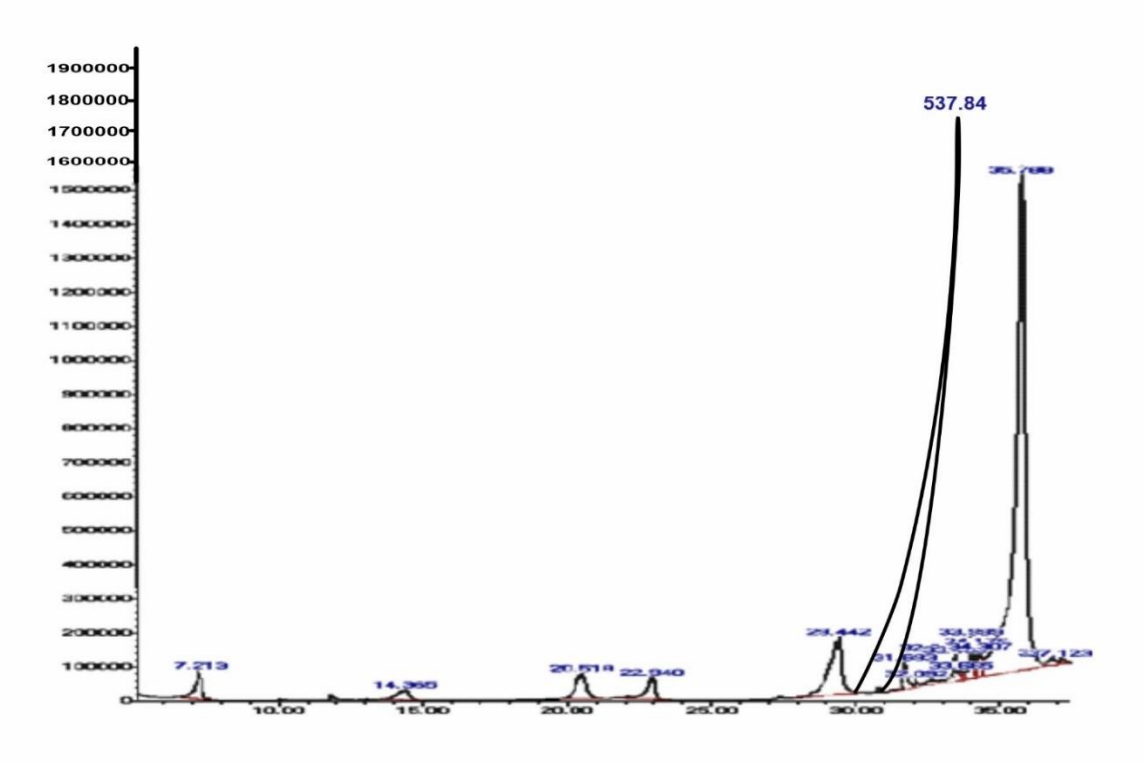

(d) GC-MS Spectrum of Sample R [$Mn(PMP)_2.Cl_2$]

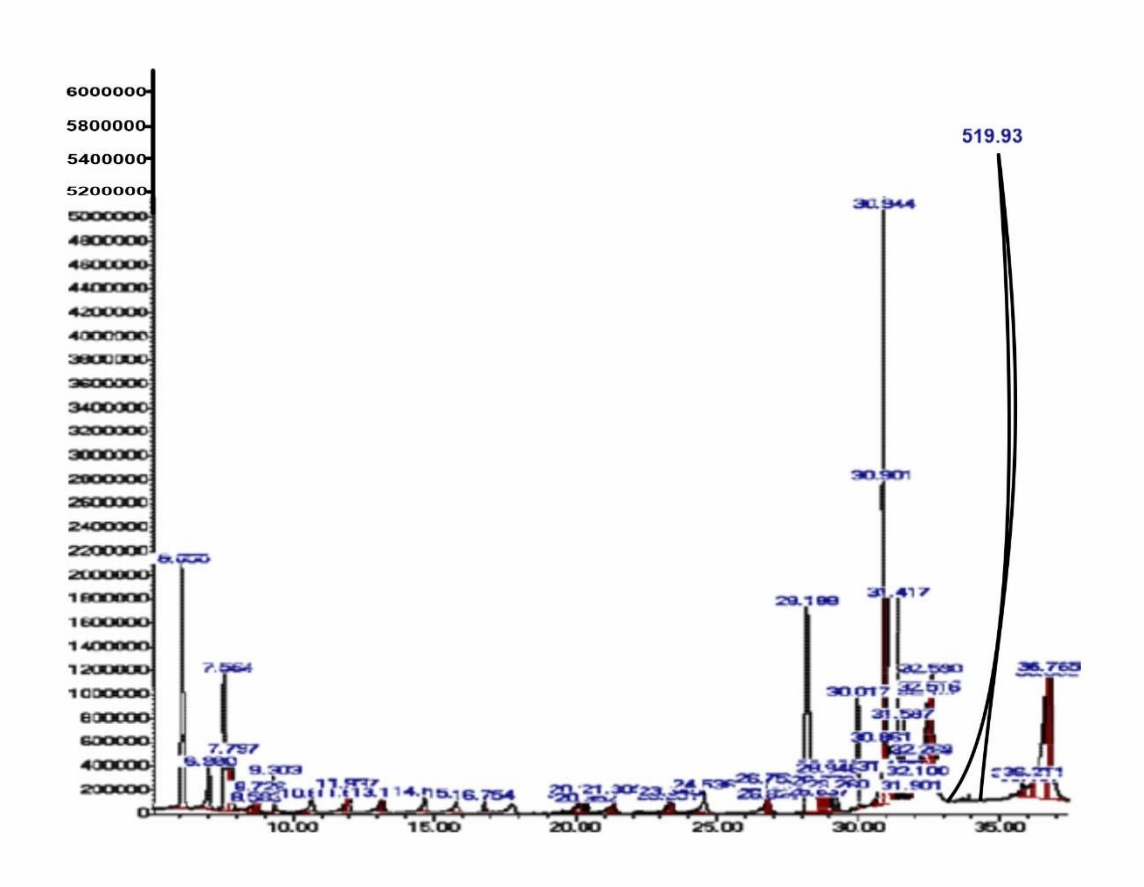

(e) GC-MS Spectrum of Sample S [$Mn(HAP)_2.Cl_2$]

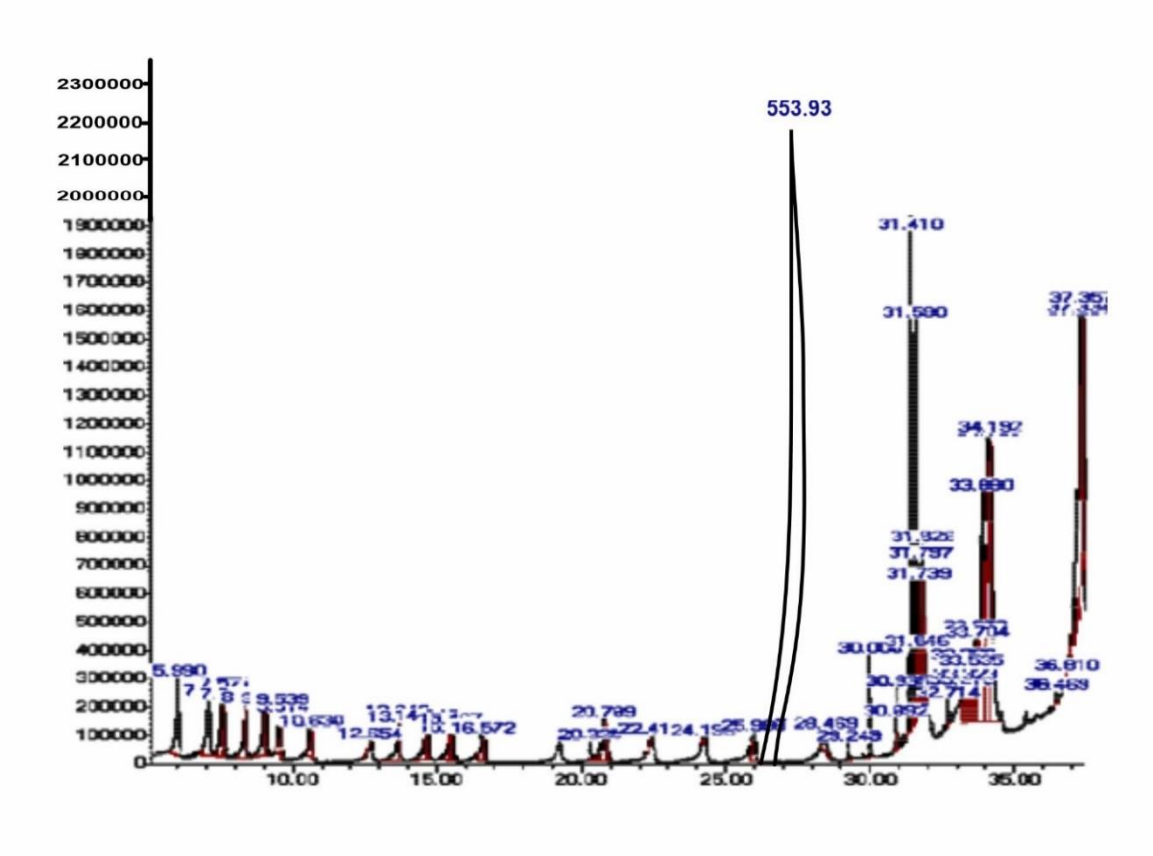

(f) GC-MS Spectrum of Sample T [$Mn(PMP+HAP).Cl_2$]

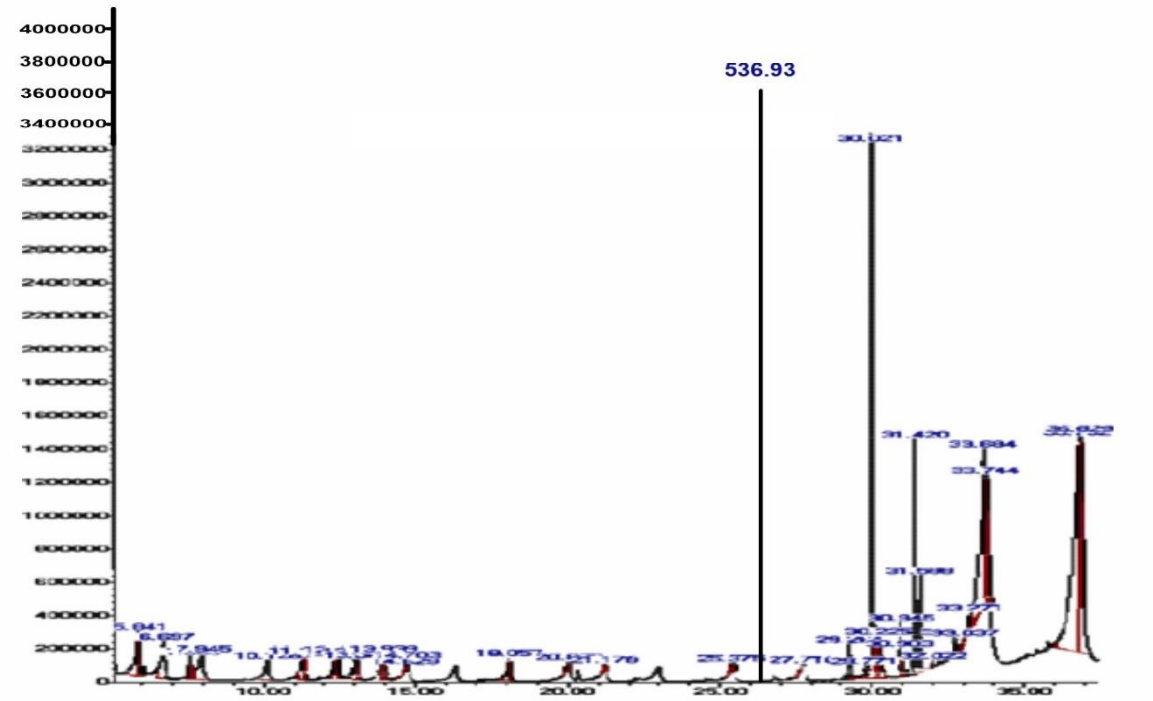

Appendix E. FTIR Spectra of Samples

(a) FTIR Spectrum of 2-Phenyliminomethylphenol (PMP) (Anumata *et al.*, 2024)

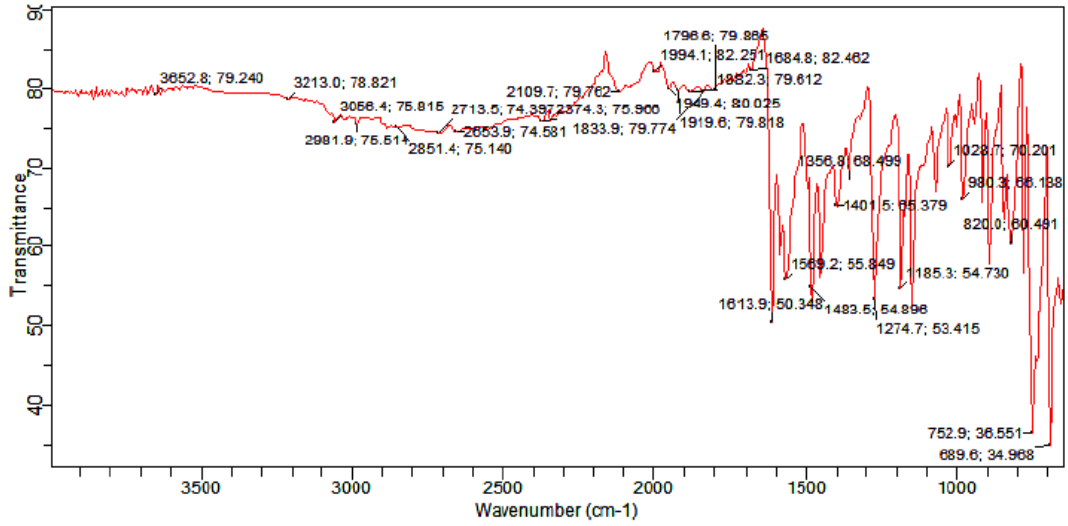

(b) FTIR Spectra of 2,2-Hydroxybenzylideneaminophenol (HAP) (Anumata *et al.*, 2024)

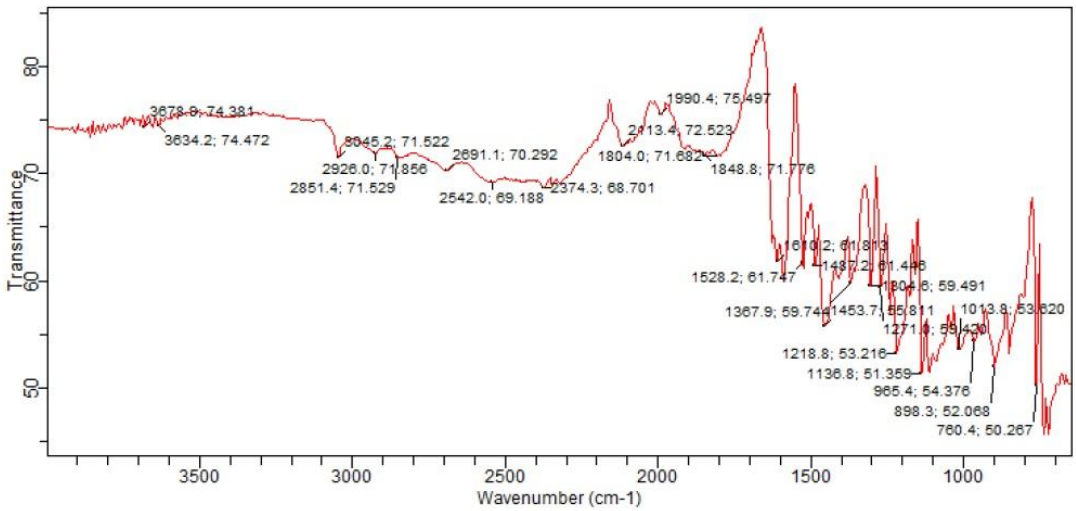

(c) FTIR Spectra of Phenyliminomethylphenol Iron(II) chloride complex, [Fe(PMP)$_2$.Cl$_2$]

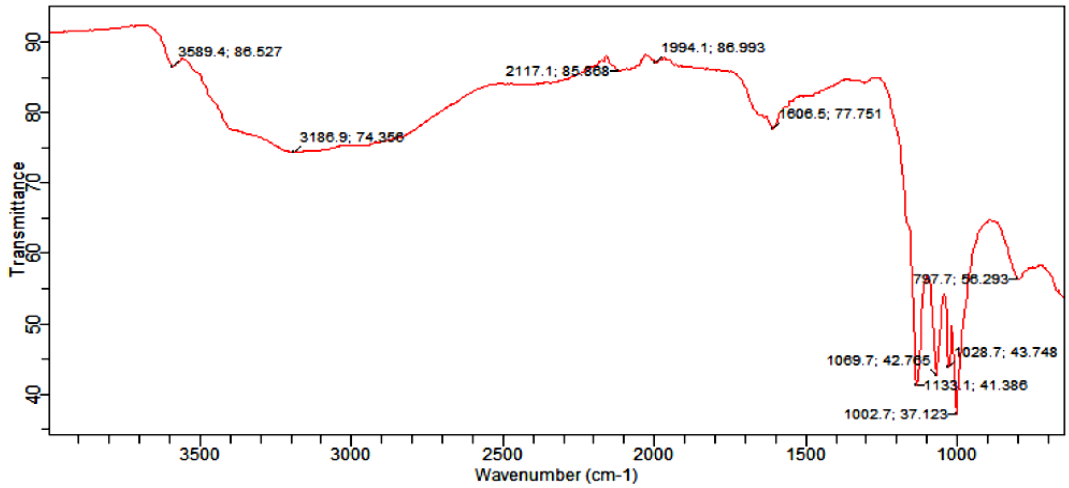

(d) FTIR Spectra of 2,2-Hydroxybenzylideneaminophenol Iron(II)chloride complex, [Fe(HAP)$_2$.cl$_2$]

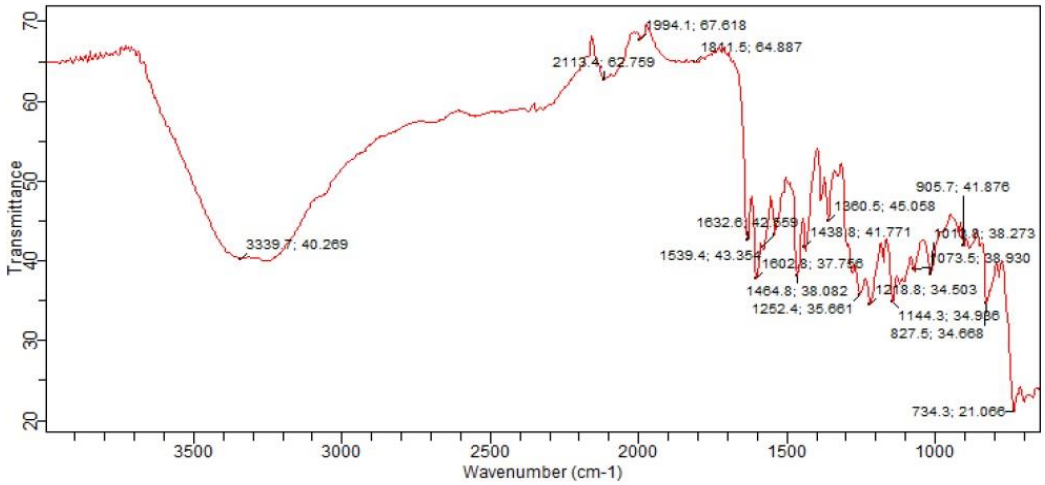

(e) FTIR Spectra of mixed ligand PMP+HAP of Iron(II)chloride complex, [Fe(PMP+HAP).cl$_2$]

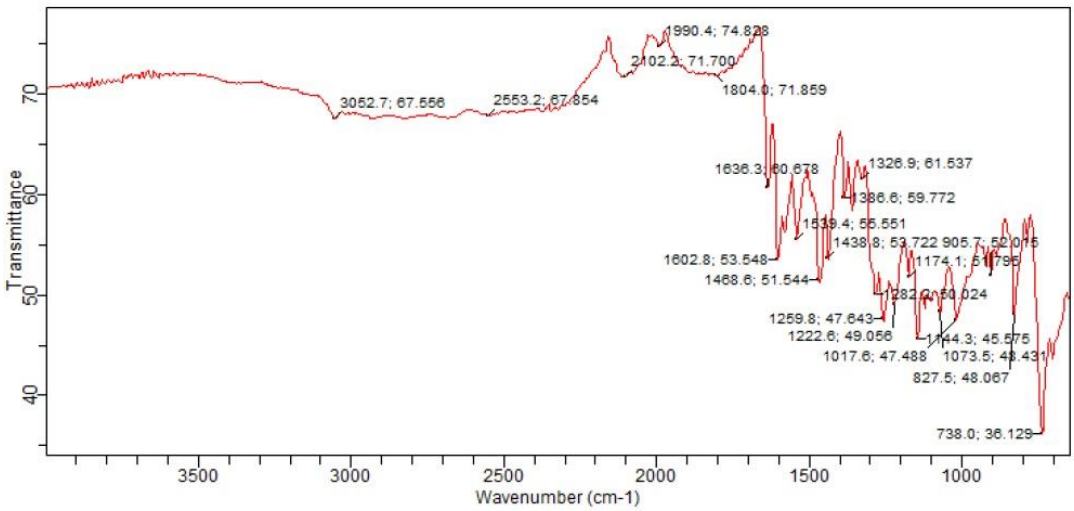

(f) FTIR Spectra of 2-Phenyliminomethylphenol Manganese(II) chloride complex, [Mn(PMP)$_2$.Cl$_2$]

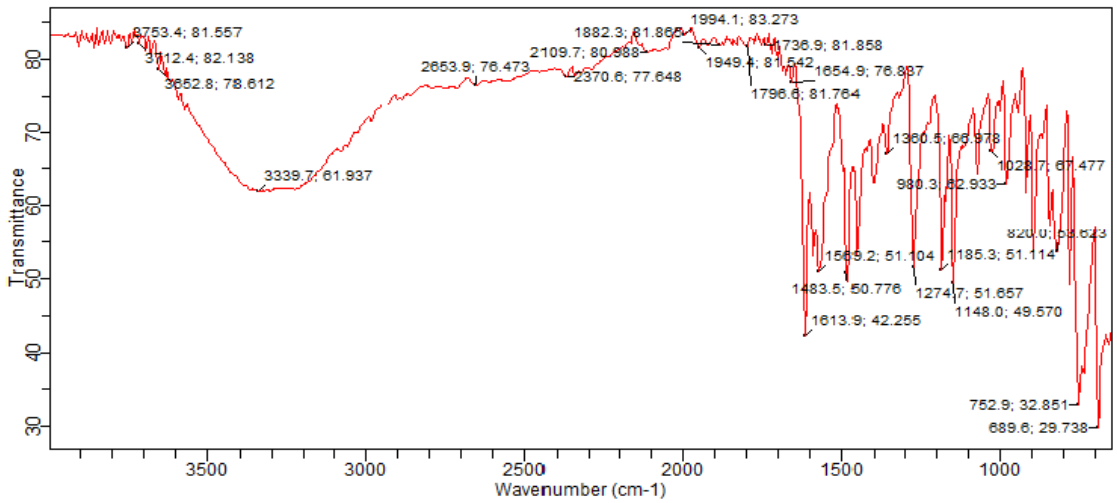

(g) FTIR Spectra of 2,2-Hydroxybenzylideneaminophenol Manganese(II) chloride complex, [Mn(HAP)$_2$.Cl$_2$]

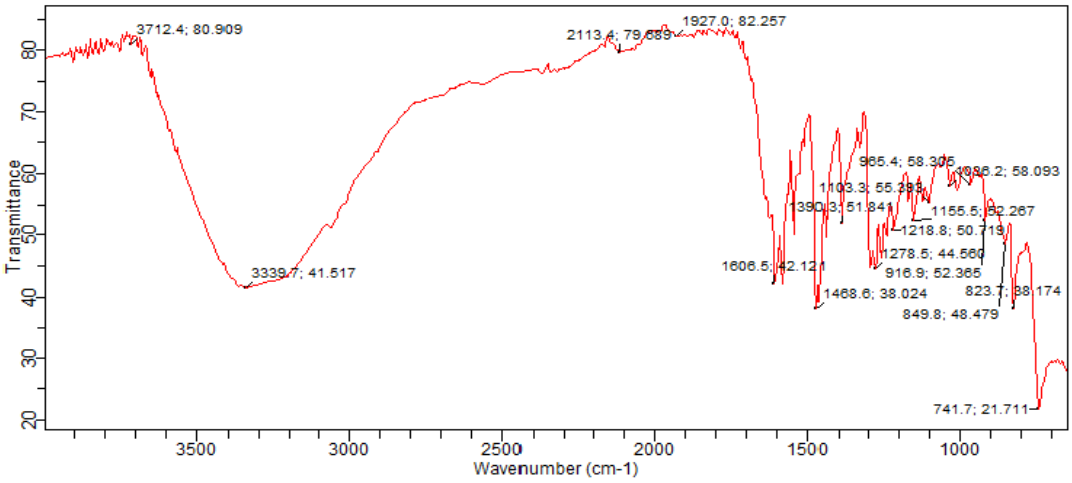

(h) FTIR Spectra for mixed ligand PMP+HAP Manganese(II) chloride complex, [Mn(PMP+HAP).Cl$_2$].

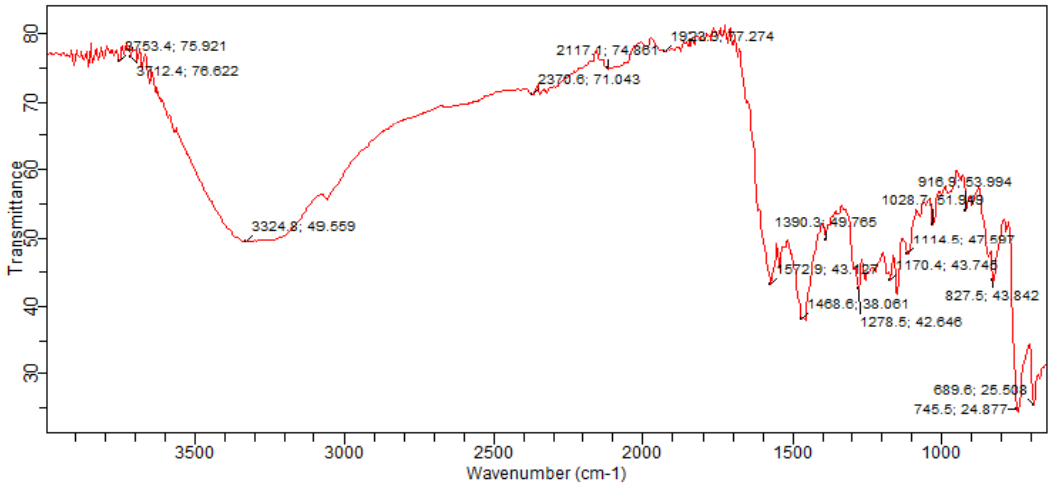

Appendix F. UV-visible Spectra of Samples

(a) F. UV-visible Spectra of 2-phenyliminomethylphenol Iron(II) Chloride Complex, [Fe(PMP)$_2$.Cl$_2$]

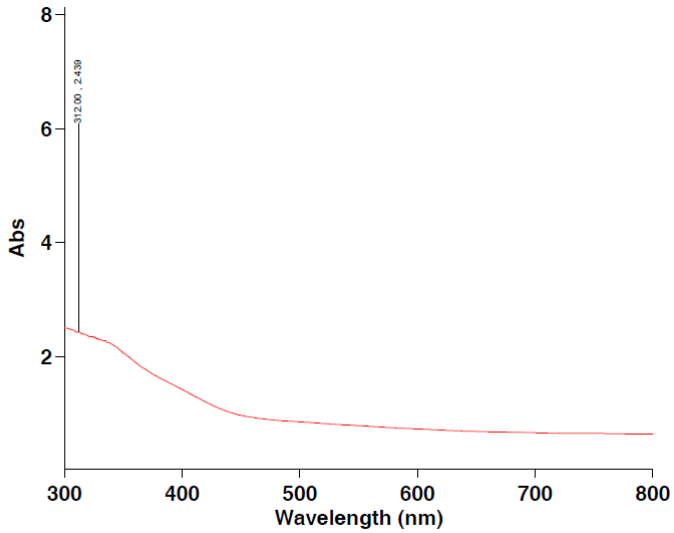

(b) UV-visible Spectra of 2,2-Hydroxybenzylideneaminophenol Iron(II) Chloride Complex, [Fe(HAP)$_2$.Cl$_2$]

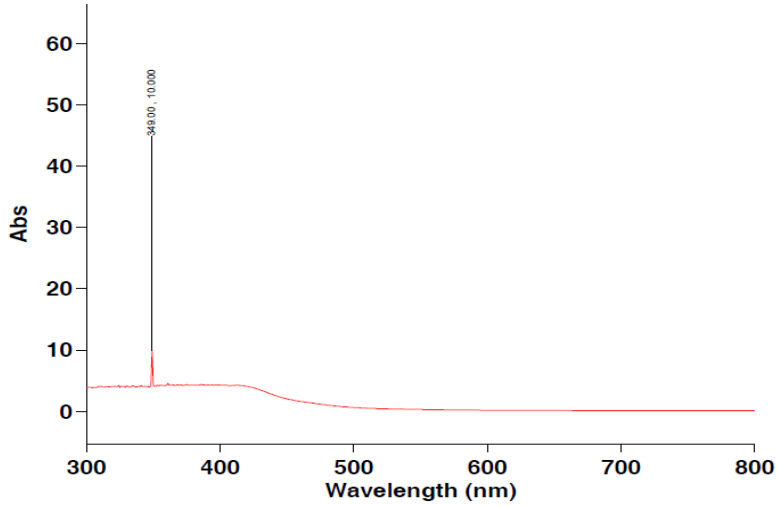

(c) UV-visible Spectra of Mixed Ligand (PMP+HAP) Iron(II) Chloride Complexes, [Fe(PMP+HAP).Cl$_2$]

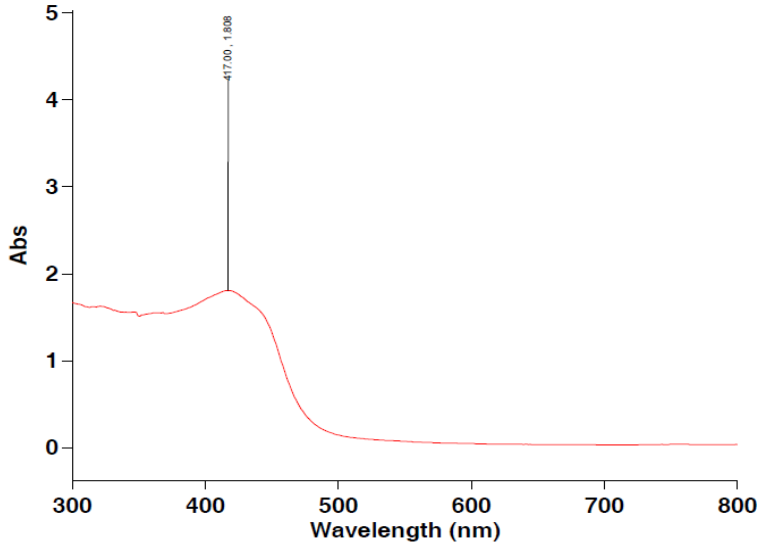

(d) UV-visible Spectra of 2-Phenyliminomethylphenol Manganese(II) Chloride Complex, [Mn(PMP)$_2$.Cl$_2$]

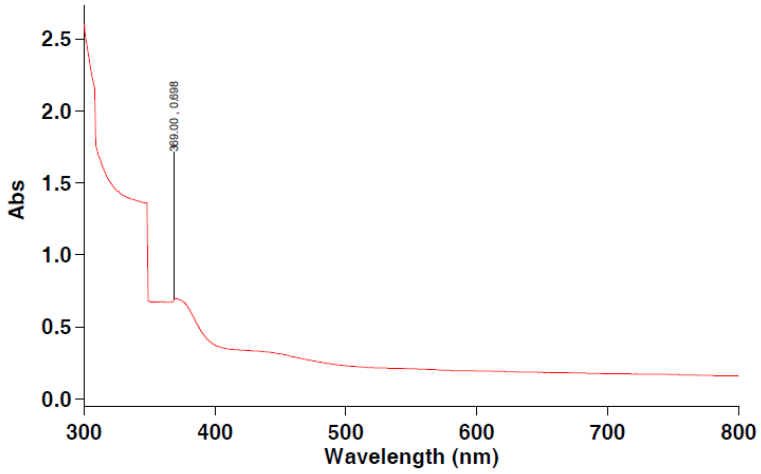

(e) UV-visible Spectra of 2,2-Hydroxybenzylideneaminophenol Manganese(II) Chloride Complex, [Mn(PMP)$_2$.Cl$_2$]

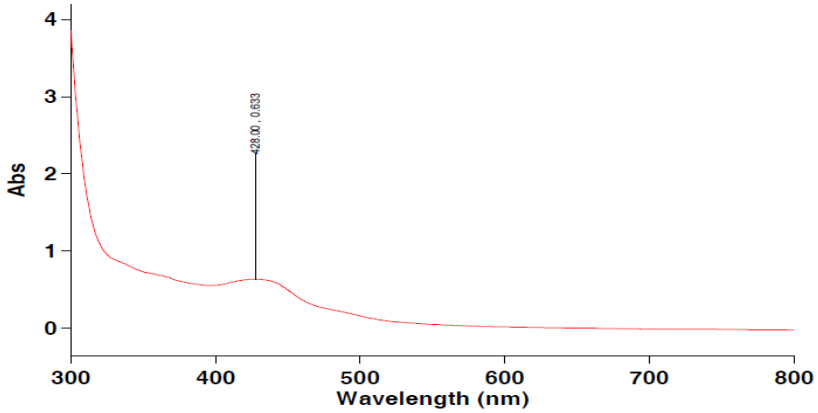

(f) UV-visible Spectra of Mixed Ligand (PMP+HAP) Manganese(II) Chloride Complex, [Mn(PMP+HAP)$_2$.Cl$_2$]

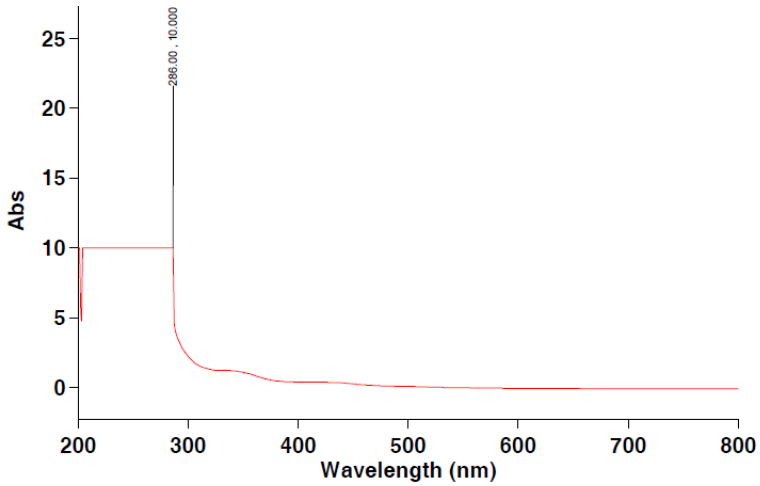

Appendix G. XRD Spectra of Ligands

(a) XRD Spectra of 2-Phenyliminomethylphenol Ligand

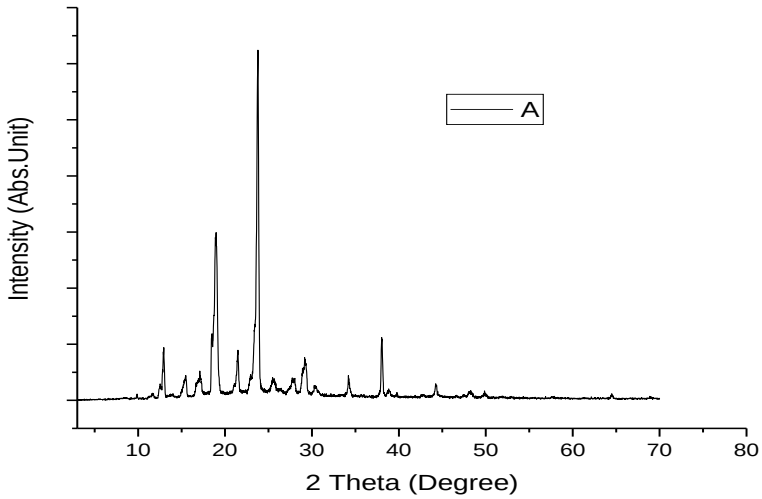

(b) XRD Spectra of 2,2-Hydroxybenzylideneaminophenol Ligand

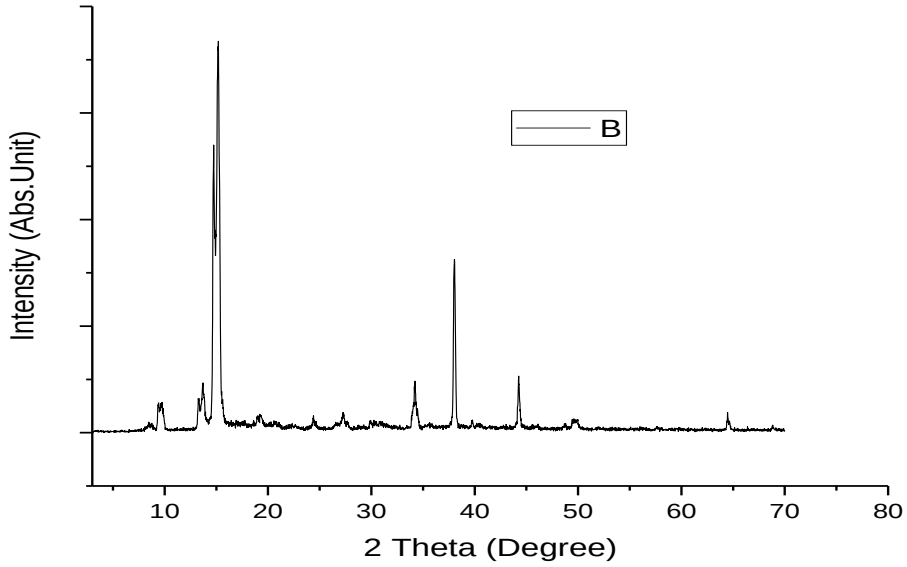

Appendix H. XRD Spectra of Samples

(a) XRD Spectra of 2-Phenyliminomethylphenol of Iron(II) Chloride Complex, [Fe(PMP)$_2$.Cl$_2$]

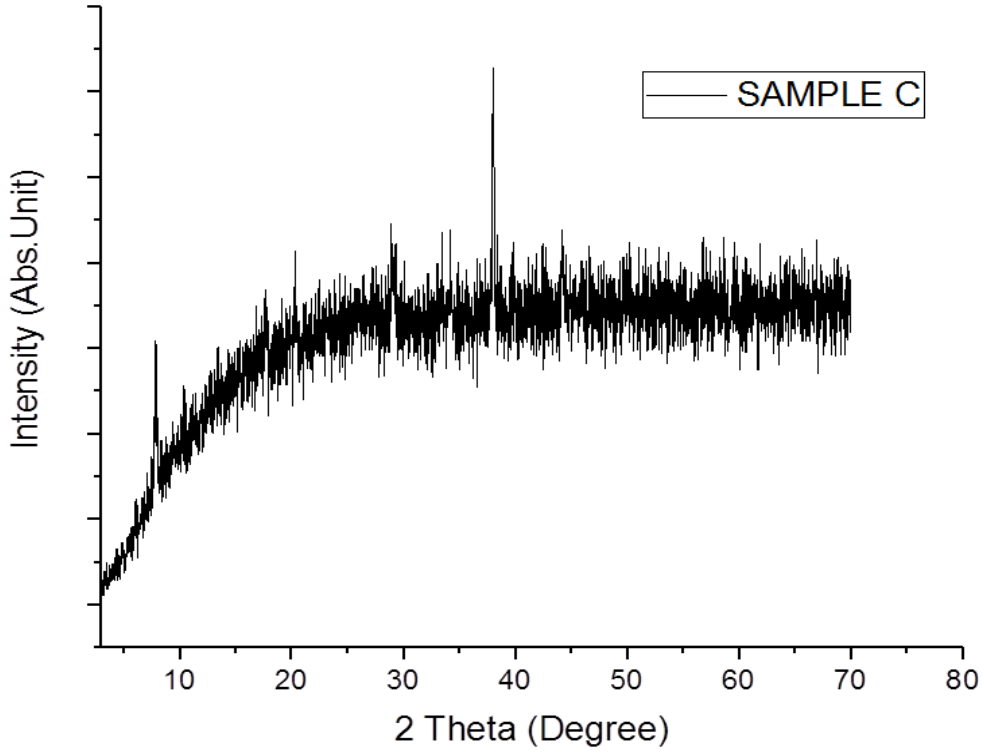

(b) XRD Spectra of 2,2-Hydroxybenzylideneaminophenol of Iron(II) Chloride Complex, [Fe(HAP)$_2$.Cl$_2$]

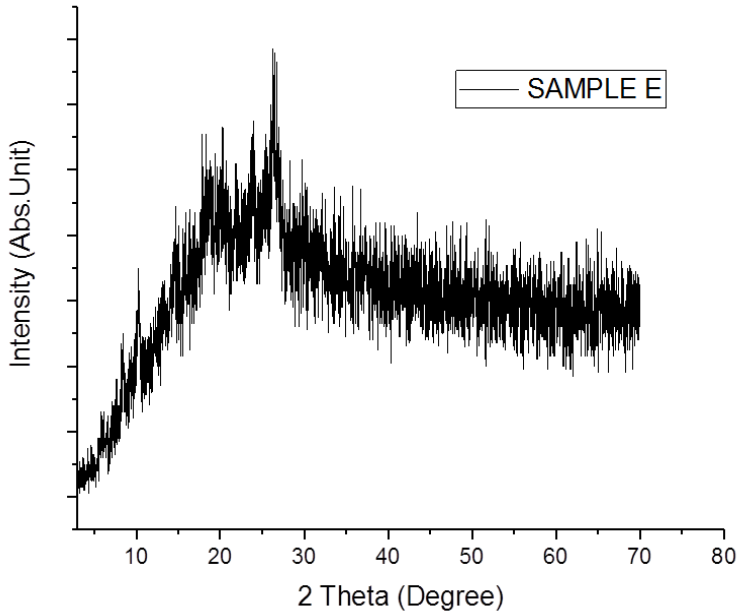

(c) XRD Spectra of Mixed Ligand (PMP+HAP) of Iron(II) Chloride Complex, [Fe(PMP+HAP).Cl$_2$]

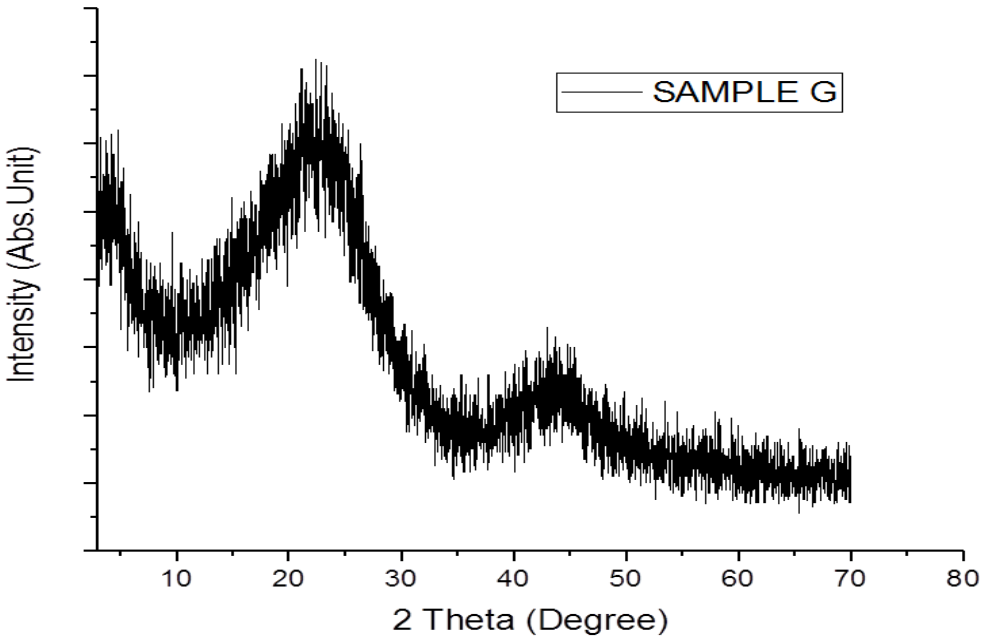

(d) XRD Spectra of 2-Phenyliminomethylphenol Manganese(II) Chloride Complex, [Mn(PMP)$_2$.Cl$_2$]

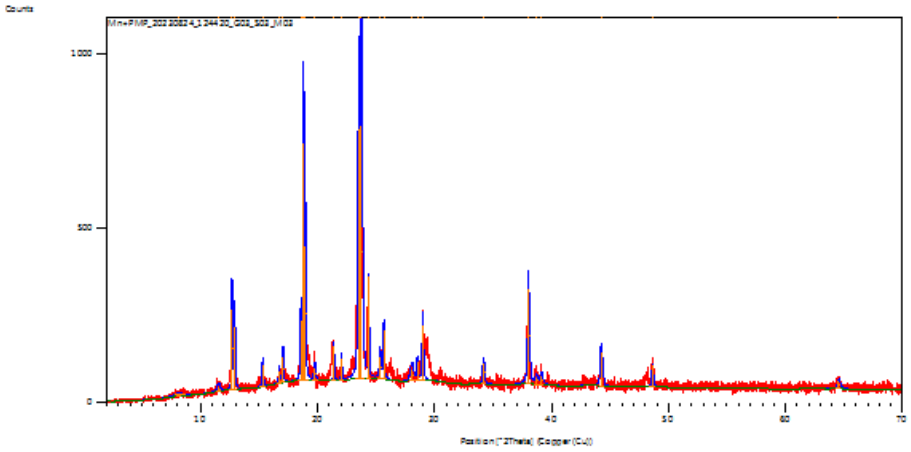

(e) XRD Spectra for 2,2-Hydroxybenzylideneaminophenol of Manganese(II) Chloride Complex, [Mn(HAP)$_2$.Cl$_2$].

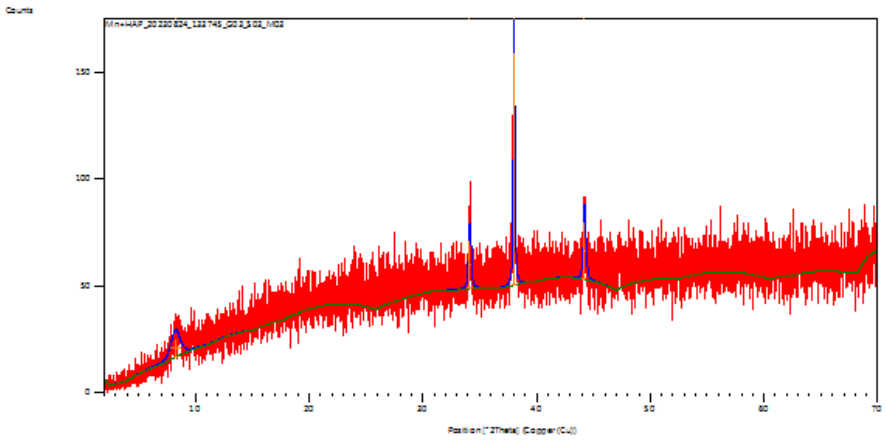

(f) XRD Spectra of Mixed Ligand (PMP+HAP) of Manganese(II) Chloride Complex, [Mn(PMP+HAP).Cl$_2$]